Up-regulated genes involved in glutathione metabolism, apoptosis, MAPK signaling pathway, and regulation of cell cycle

The individual gene expression change (ratio to control) in each category was depicted as heatmap (Fig. 3 to 6) for "glutathione metabolism", "apoptosis", "MAPK signaling" and "regulation of cell cycle", respectively. In general, most of the genes were dose-dependently mobilized and characteristic changes were noticed in single and repeated dosing groups. As for genes involved in glutathione biosynthesis: glutamate cysteine ligase, modifier subunit (Gclm) and glutamate-cysteine ligase, catalytic subunit (Gclc) (Fig. 3); those involved in the regulation of apoptosis: v-akt murine thymoma viral oncogene homolog 1 (Akt1) and programmed cell death 6 interacting protein (Pdcd6ip) (Fig. 4), and those belonging to heat shock proteins: heat shock 70 kD protein 1A/1B (Hspa1a/1b) and heat shock protein 8 (Hspa8) (Fig. 5), these were markedly up-regulated in the early stage of single dose, whereas little or no changes were noted in repeated dosing. Excluding these genes, the extent of up-regulation increased with repeated administration in most of the genes. Especially, those involved in glutathione metabolism: glucose-6-phosphate dehydrogenase (G6pdx), glutathione *S*-transferase M4 (Gstm4) and glutathione *S*-transferase Yc2 subunit (Yc2) (Fig. 3), those involved in regulation of apoptosis: nucleolar protein 3 (Nol3), rhoB gene (Rhob) and tribbles homolog 3 (Drosophila) (Trib3) (Fig. 4), those belonging to MAPK signaling and known as cell cycle regulators: myelocytomatosis viral oncogene homolog (avian) (Myc),

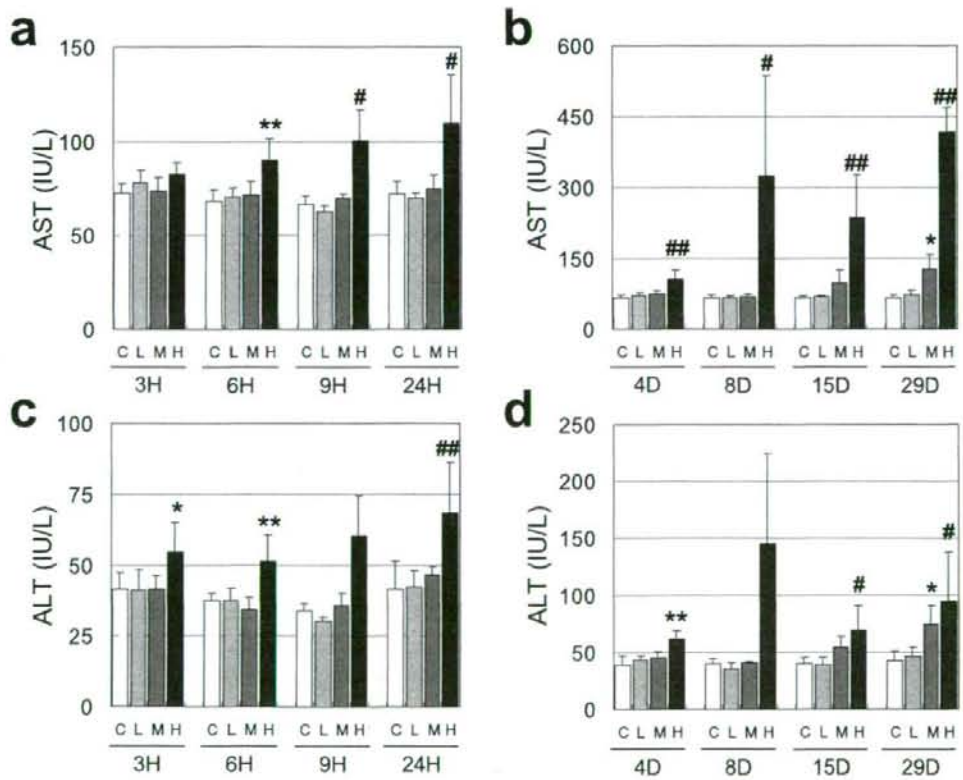

Fig. 1. Serum AST (a and b) and ALT activities (c and d) in rats treated with 10, 30 and 300 mg/kg MP in single and repeated dose studies.
Data are expressed as mean ± S.D. (n = 5). *, **Significant difference from the control group, $p < 0.05, 0.01$, by Dunnett's multiple comparison test. #,##Significant difference from the control group, $p < 0.05, 0.01$, by Mann-Whitney's U test.

Table 1. Histopathological findings in rat liver treated with MP in single dose study.

Morphology	Time Point (hrs)	3			6			9			24		
	Dose (mg/kg)	10	30	100	10	30	100	10	30	100	10	30	100
	Number of animals examined	5	5	5	5	5	5	5	5	5	5	5	5
Hepatocyte / Anisonucleosis		0	0	0	0	0	0	0	0	0	0	0	5
slight													5
Hepatocyte / Hypertrophy		0	0	1	0	0	3	0	0	4	0	1	5
slight				1			3			4		1	5
Hepatocyte / Single cell necrosis		0	0	1	0	0	3	0	0	5	0	0	5
slight				1			3			5			5
Periportal / Cellular infiltration, mononuclear cell		0	0	0	0	0	0	0	0	5	0	0	5
slight										5			5

Vehicle alone, or MP 10, 30, or 100 mg/kg was administered orally to rats, and the animals were euthanized at 3, 6, 9 and 24 hr after dosing (n = 5). The histopathological change in liver was graded into 4 categories: very slight, slight, moderate, and severe. The number of animals affected at each grade is shown.

Table 2. Histopathological findings in rat liver treated with MP in repeated dose study.

Morphology	Time Point (days)	4			8			15			29		
	Dose (mg/kg)	10	30	100	10	30	100	10	30	100	10	30	100
	Number of animals examined	5	5	5	5	5	5	5	5	5	5	5	4[a]
Hepatocyte / Alteration, cytoplasmic		0	0	0	0	0	0		0	0	0	0	1
slight													1
Hepatocyte / Anisonucleosis		0	0	3	0	0	4		0	5	0	0	4
slight				3			4			5			4
Hepatocyte / Hyperplasia		0	0	0	0	0	0		0	0	0	0	4
slight													4
Hepatocyte / Hypertrophy		0	2	5	1	2	5		3	5	1	5	4
slight			2	5	1	2	5		3	5	1	5	4
Hepatocyte / Increased mitosis		0	1	4	0	0	3		1	0	0	3	3
slight			1	4			3		1			3	3
Hepatocyte / Single cell necrosis		0	0	5	0	0	5		3	5	0	3	4
slight				5			5		3	5		3	4
Interlobular / Proliferation, bile duct		0	0	5	0	0	5		1	5	0	0	4
slight				5			5		1	4			
moderate										1			4
Periportal / Cellular infiltration, mononuclear cell		0	1	4	0	0	4		5	5	0	2	4
slight			1	4			4		5	2		2	4
moderate										3			
Periportal / Deposit, pigment		0	0	0	0	0	0		0	0	0	0	3
slight													3

Vehicle alone, or MP 10, 30, or 100 mg/kg was administered orally to rats once daily for 1, 3, 7, 14, and 28 days, and the animals were euthanized at 24 hr after dosing, namely, on 2, 4, 8, 15, and 29 days (n = 5). [a]One of the 5 rats died and was not examined histopathologically due to advanced autolysis. For more detailed information, see Table 1.

FBJ murine osteosarcoma viral oncogene homolog (Fos), v-jun sarcoma virus 17 oncogene homolog (avian) (Jun) and fibroblast growth factor 21 (Fgf21) (Fig. 5), and those related to DNA damage: growth arrest and DNA-damage-inducible 45 alpha (Gadd45a) and DNA-damage inducible transcript 3 (Ddit3) (Fig. 6), these kept up-regulated throughout the repeated dosing periods.

DISCUSSION

Methapyrilene hydrochloride is an antihistamine drug and had been used in the 1970s, but was removed from the market once it was known to be carcinogenic in rat liver (Lijinsky *et al.*, 1980; Fischer *et al.*, 1983). It is now considered to be a rat-specific carcinogen since hepatocellular carcinoma and cholangiocarcinoma were induced by administration of MP at 1000 ppm for 64 weeks, whereas no such findings were observed either in Syrian hamsters, Guinea-pigs, B6C3F1 mice, or humans (Mirsalis, 1987). As for its genotoxicity, the Ames test, DNA addition test, chromosome abnormality test (NTP, 2000) and irregular DNA synthesis test in rat and mouse (Steinmetz *et al.*, 1988) were all negative, whereas the cell transformation assay and L5178Y/TK+/− mouse lymphoma assay were positive (Turner *et al.*, 1987). Based on these observations, hepatocarcinogenicity of MP in rat has been considered to be non-genotoxic, whereas the involvement of its initiation activity cannot be completely excluded (Althaus *et al.*,

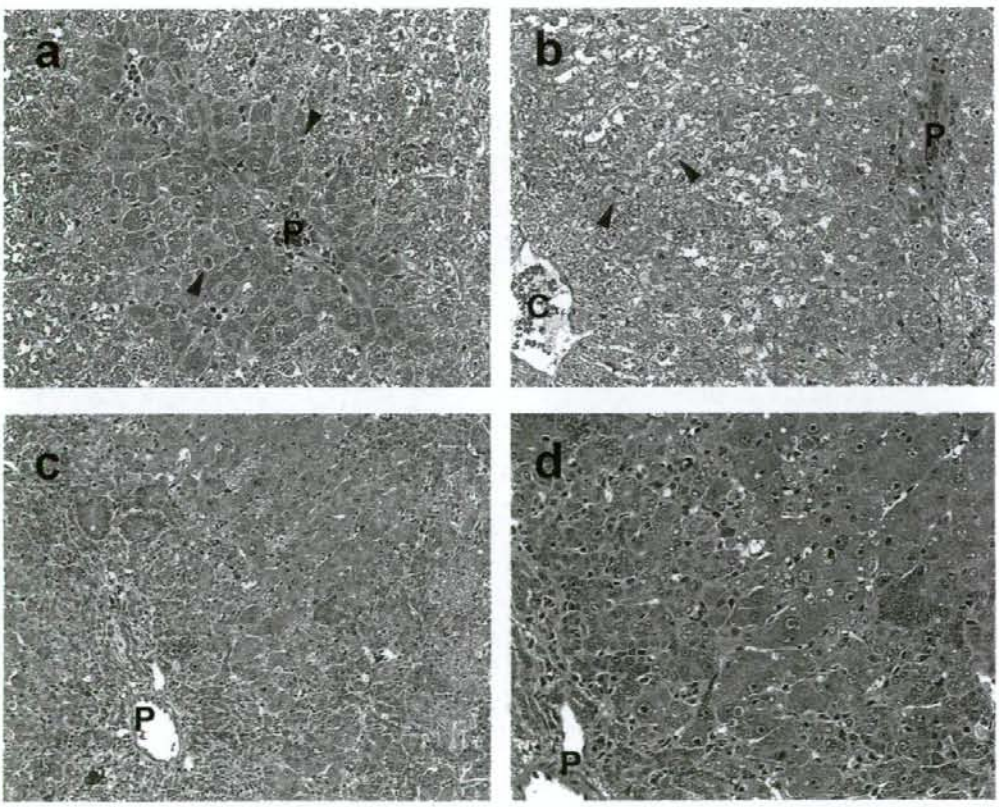

Fig. 2. Histopathological changes of liver treated with 100 mg/kg MP.
a: Hepatocellular hypertrophy and single cell necrosis (arrow head) in the periportal region (P) are observed at early time point, 24 hr after single dosing. b: Additional regenerative changes, such as increased mitosis, bile duct proliferation, and hyperplasia are evident by repeated administration.

Table 3. Gene ontology and pathway classification of extracted probe sets (up-regulation).

Exp. type	TERM[a]	Count[b]	p value[c]
Single dose study			
	GOTERM_BP_5		
	REGULATION OF NUCLEOBASE, NUCLEOSIDE, NUCLEOTIDE AND NUCLEIC ACID METABOLISM	18	6.41E-2
	TRANSCRIPTION	18	7.48E-2
	MACROMOLECULE BIOSYNTHESIS	**13**	**1.92E-2**
	PROTEIN BIOSYNTHESIS	**11**	**3.84E-2**
	REGULATION OF CELL CYCLE	**11**	**5.95E-4**
	INTRACELLULAR TRANSPORT	**9**	**8.5E-2**
	AMINO ACID METABOLISM	6	2.75E-2
	AMINE BIOSYNTHESIS	5	9.11E-3
	CELL GROWTH	5	4.86E-2
	NUCLEAR TRANSPORT	5	2.6E-3
	NUCLEOCYTOPLASMIC TRANSPORT	5	6.12E-3
	PROTEIN KINASE CASCADE	5	4.18E-2
	REGULATION OF CELL SIZE	5	4.86E-2
	RNA METABOLISM	5	4.63E-2
	POSITIVE REGULATION OF NUCLEOBASE, NUCLEOSIDE, NUCLEOTIDE AND NUCLEIC ACID METABOLISM	4	8.74E-2
	PROTEIN IMPORT	4	1.49E-2
	RNA PROCESSING	4	6E-2
	GOTERM_CC_5		
	NUCLEUS	34	7.29E-3
	KEGG_PATHWAY		
	MAPK SIGNALING PATHWAY (Rattus norvegicus)	**10**	**3.73E-2**
	GAP JUNCTION (Rattus norvegicus)	6	5.15E-2
	TGF-BETA SIGNALING PATHWAY (Rattus norvegicus)	5	8.22E-2
	ARGININE AND PROLINE METABOLISM (Rattus norvegicus)	4	3.69E-2
	GLUTATHIONE METABOLISM (Rattus norvegicus)	**4**	**2.42E-2**
Repeated dose study			
	GOTERM_BP_5		
	CELLULAR PROTEIN METABOLISM	189	2.86E-8
	MACROMOLECULE BIOSYNTHESIS	**89**	**4.92E-17**
	PROTEIN BIOSYNTHESIS	**85**	**2.13E-19**
	INTRACELLULAR TRANSPORT	**60**	**1.22E-9**
	PROTEIN TRANSPORT	47	1.48E-6
	INTRACELLULAR PROTEIN TRANSPORT	44	4.84E-7
	APOPTOSIS	38	3.07E-4
	REGULATION OF CELL CYCLE	**32**	**6.48E-4**
	REGULATION OF APOPTOSIS	31	2.99E-4
	REGULATION OF PROGRAMMED CELL DEATH	31	3.48E-4
	GOTERM_CC_5		
	VESICLE-MEDIATED TRANSPORT	30	1.48E-2
	CYTOSKELETON	64	6.02E-2
	RIBOSOME	60	1E-13
	MICROTUBULE CYTOSKELETON	41	2.59E-3
	KEGG_PATHWAY		
	MICROTUBULE ASSOCIATED COMPLEX	29	6.25E-2
	CYTOSOLIC RIBOSOME (SENSU EUKARYOTA)	26	2.79E-11
	RIBOSOME (Rattus norvegicus)	40	1.79E-24
	FOCAL ADHESION (Rattus norvegicus)	36	6.68E-2
	MAPK SIGNALING PATHWAY (Rattus norvegicus)	**33**	**7.61E-2**
	TIGHT JUNCTION (Rattus norvegicus)	27	4.25E-3
□y	**GLUTATHIONE METABOLISM (Rattus norvegicus)**	**8**[d]	**4.55E-2**

Pathway and GO analysis was performed using David 2.1 beta. Statistical significant terms are listed (Fisher's exact test, $p < 0.05$; threshold counts: greater than 10% of the number of probe sets involved in the examined gene list). Bold terms were commonly affected in both single and repeated dose studies. Shaded terms were further analyzed by scoring based on the TGP1-score.

Table 4. Gene ontology and pathway classification of extracted probe sets (up-regulation).

Exp. type	TERM[a]	Count[b]	p value[c]
Single dose study			
	GOTERM_BP_5		
	REGULATION OF NUCLEOBASE, NUCLEOSIDE, NUCLEOTIDE AND NUCLEIC ACID METABOLISM	13	9.72E-2
	REGULATION OF TRANSCRIPTION	13	9.51E-2
	RESPONSE TO CHEMICAL SUBSTANCE	4	8.4E-2
	CHEMOTAXIS	3	5.47E-2
	STEROL METABOLISM	3	6.27E-2
	KEGG_PATHWAY		
	STARCH AND SUCROSE METABOLISM (Rattus norvegicus)	3	4.97E-2
Repeated dose study			
	GOTERM_BP_5		
	CARBOXYLIC ACID METABOLISM	45	2.26E-16
	ELECTRON TRANSPORT	37	2.19E-8
	CELLULAR LIPID METABOLISM	34	7.06E-8
	IMMUNE RESPONSE	27	5.94E-2
	RESPONSE TO PEST, PATHOGEN OR PARASITE	21	4.78E-5
	AMINO ACID METABOLISM	20	1.32E-7
	CELLULAR CARBOHYDRATE METABOLISM	18	1.36E-3
	LIPID BIOSYNTHESIS	15	2.41E-3
	STEROID METABOLISM	15	1.6E-5
	WOUND HEALING	14	4.27E-5
	BLOOD COAGULATION	13	2.03E-6
	FATTY ACID METABOLISM	13	2.59E-3
	MONOSACCHARIDE METABOLISM	13	3.96E-3
	AMINO ACID DERIVATIVE METABOLISM	12	2.04E-4
	COENZYME METABOLISM	12	1.31E-2
	COFACTOR BIOSYNTHESIS	11	1.7E-2
	COMPLEMENT ACTIVATION	11	1.28E-7
	HUMORAL IMMUNE RESPONSE	11	3.22E-6
	AMINE CATABOLISM	10	1.37E-5
	RESPONSE TO CHEMICAL SUBSTANCE	10	2.22E-2
	INFLAMMATORY RESPONSE	9	3.47E-2
	GOTERM_CC_5		
	MITOCHONDRION	38	2.07E-5
	ENDOPLASMIC RETICULUM	26	8.26E-6
	MICROSOME	18	5.64E-7
	KEGG_PATHWAY		
	TRYPTOPHAN METABOLISM (Rattus norvegicus)	22	5.32E-12
	COMPLEMENT AND COAGULATION CASCADES (Rattus norvegicus)	17	7.4E-7
	FATTY ACID METABOLISM (Rattus norvegicus)	17	3.65E-7
	GLYCINE, SERINE AND THREONINE METABOLISM (Rattus norvegicus)	11	5.69E-7
	BUTANOATE METABOLISM (Rattus norvegicus)	9	7.11E-4
	GAMMA-HEXACHLOROCYCLOHEXANE DEGRADATION (Rattus norvegicus)	9	1.29E-3
	LYSINE DEGRADATION (Rattus norvegicus)	9	1.26E-5
	PYRUVATE METABOLISM (Rattus norvegicus)	9	3.61E-4
	STARCH AND SUCROSE METABOLISM (Rattus norvegicus)	**9**	**1.08E-4**
□y	VALINE, LEUCINE AND ISOLEUCINE DEGRADATION (Rattus norvegicus)	9	3.61E-4

1982).

The analysis of hepatotoxicity of MP has been repeatedly performed by various techniques including the toxicogenomics approach (Hamadeh *et al.*, 2002). This compound induces marked and reproducible hepatic injury in rodents, and was used to assess the validity of toxicogenomics analyses among the multicenter platform (Waring *et al.*, 2004; Chu *et al.*, 2004). In the former study, there was a pessimistic interpretation that microarrays never supply highly reliable measures because of too large variance between research facilities. In this case, samples from the same animal were analyzed in multiple facilities but there were almost no genes that were detected as commonly changed in all the facilities. However, the latter study revealed that the robustness of the results regarding the movement of certain toxicological pathways was sufficient although the fitness of each gene was somewhat questionable. In other words, when we have a reasonable list of genes with certain toxicological significance, the reliability would be highly improved. The strategy of our project follows this idea, i.e., the results are interpreted as a trend for a set of functional genes.

Presently extracted genes from the group receiving the highest dose (showing obvious phenotypes) were categorized and this revealed that genes related to the regulation of cell cycle, MAPK signaling, and the glutathione metabolism were all involved in the development of the presently observed phenotypes. As for the down-regulated genes in repeated dosing, it could be a reflection of the failure of hepatic functions, *i.e.*, metabolism of sugar and sterols, and production of functional proteins such as complements and blood coagulation.

To facilitate the analytical procedures for our large-scale microarray database, we developed two types of the one-dimensional score, named as TGP1 and TGP2, which express the trend of the changes in expression of biomarker genes as a whole. The former is based on the signal log ratio (Kiyosawa *et al.*, 2006) and is convenient to compare the responsiveness of many drugs to a marker gene list. The disadvantages of this scoring system are that it overestimates the responsiveness when the list contains a gene where the induction is extreme (such as CYP1A1) and it

Table 5. Time course changes of TGP-1 scores in selected MP-responsive gene lists.

MP-RESPONSIVE GENE LISTS	03H			06H			09H			24H		
	L	M	H	L	M	H	L	M	H	L	M	H
GLUTATHIONE METABOLISM	23	2	7	2	39	607	−2	24	498	−35	−1	409
APOPTOSIS	6	7	103	3	24	342	8	10	128	0	2	195
MAPK SIGNALING PATHWAY	3	9	190	−2	7	114	−5	−26	15	−5	−2	57
REGULATION OF CELL CYCLE	3	2	108	−2	5	133	−3	−1	33	−3	−2	21
MP-RESPONSIVE GENE LISTS	04D			08D			15D			29D		
	L	M	H	L	M	H	L	M	H	L	M	H
GLUTATHIONE METABOLISM	2	118	476	2	170	3466	0	235	2285	5	712	2865
APOPTOSIS	2	54	286	93	227	1172	3	154	1360	−4	115	1396
MAPK SIGNALING PATHWAY	13	3	34	13	60	295	3	68	354	7	29	378
REGULATION OF CELL CYCLE	10	4	7	13	20	219	1	15	247	4	28	470

AFFYMETRIX PROBE ID	SYMBOL	03H			06H			09H			24H			04D			08D			15D			29D		
		L	M	H	L	M	H	L	M	H	L	M	H	L	M	H	L	M	H	L	M	H	L	M	H
1367856_at	G6pdx	1.1	0.9	0.9	1.2	1.4	2.5	1.1	1.5	4.2	1.0	1.4	2.9	1.4	0.8	1.4	0.6	0.9	1.8	1.1	1.2	3.9	1.0	0.8	5.0
1368374_a_at	Ggt1	1.1	1.0	0.9	1.1	0.9	0.7	1.0	0.7	0.9	1.0	1.2	1.3	1.0	1.0	1.3	1.3	1.4	2.8	1.1	1.3	4.5	0.9	1.3	8.0
1369061_at	Gsr	1.2	1.1	1.2	1.1	1.5	1.8	1.2	1.8	2.7	0.9	1.2	1.7	0.9	1.2	1.2	1.0	1.2	2.1	0.8	1.0	1.6	0.9	1.2	1.9
1369921_at	Gstm4	1.1	1.1	1.1	1.2	2.0	12	0.7	1.1	6.9	0.4	0.7	6.6	1.2	4.6	7.7	1.1	1.0	63	0.7	5.0	30	1.3	8.8	8.5
1369926_at	Gpx3	1.1	1.0	0.9	1.2	1.0	1.1	0.8	0.9	0.8	0.9	0.9	0.9	1.0	1.0	0.8	0.9	0.9	2.0	1.0	1.1	2.9	1.1	1.3	9.1
1370030_at	Gclm	1.1	1.2	1.3	1.2	1.4	2.5	1.2	1.8	2.1	0.9	0.7	1.0	1.1	1.3	1.0	1.1	1.0	1.6	1.0	1.2	1.3	0.9	0.8	1.0
1370365_at	Gss	1.4	1.1	1.2	1.0	1.3	1.2	0.9	1.0	1.2	1.1	1.1	2.1	0.9	1.1	1.6	0.7	0.9	2.0	1.0	1.1	2.7	1.0	1.2	2.4
1371089_at	Yc2	2.4	1.3	1.4	1.0	1.8	2.8	0.9	1.4	3.9	0.7	1.2	5.6	0.9	1.9	6.7	1.7	5.9	30	1.4	4.6	20	1.7	11	34
1372523_at	Gclc	1.4	1.4	1.7	1.4	2.4	3.6	1.4	2.2	3.8	1.0	0.9	1.4	0.9	1.2	1.3	1.0	1.1	1.1	1.0	1.1	1.0	0.9	1.0	1.0
1374070_at	Gpx2	1.3	0.9	1.0	1.2	1.0	1.8	0.7	0.6	1.5	0.9	1.0	1.3	1.4	1.2	2.0	1.4	1.1	3.7	1.2	1.3	3.4	1.3	1.6	13

The number in each column expresses the ratio to control (N=3).

Fig. 3. Heatmap of individual gene expression change in category of "glutathione metabolism".

also underestimates the responsiveness when the genes in the list are mobilized to either direction. To overcome these disadvantages, we employed another score, TGP2, based on the effect size. In the present study, we employed the TGP1 score for assessment of the responsiveness to the gene lists, *i.e.*, "regulation of cell cycle", "MAPK signaling" and "glutathione metabolism" since the direction of expression changes was uniform. In the highest dose group, the scores for these categories markedly increased from the early time point after single dose and kept their high expression throughout the repeated dose period. In the middle dose groups, the increment of the scores were noted not only at the time points when apparent pathological changes emerged, but also at the earlier stage of repeated dosing and even after single dosing. This indicates that the toxicogenomics approach enables more sensitive assessment at the earlier time point than classical toxicology evaluation. Among the responding genes, glutathione-related: glucose-6-phosphate dehydrogenase (G6pdx), glutathione *S*-transferase M4 (Gstm4) and glutathione *S*-transferase Yc2 subunit (Yc2), apoptosis related: nucleolar protein 3 (Nol3), rhoB gene (Rhob) and tribbles homolog 3 (Drosophila) (Trib3), MAPK signaling-related: myelocytomatosis viral oncogene homolog (avian) (Myc), FBJ murine osteosarcoma viral oncogene homolog (Fos), v-jun sarcoma virus 17 oncogene homolog (avian) (Jun) and fibroblast growth factor 21 (Fgf21), and DNA damage-related: growth arrest and DNA-damage-inducible 45 alpha (Gadd45a) and DNA-damage inducible transcript 3 (Ddit3), these were markedly up-regulated from the early point of dosing. Especially, Trib3, which showed typical changes in the present study, would be one

AFFYMETRIX PROBE ID	SYMBOL	03H			06H			09H			24H			04D			08D			15D			29D		
		L	M	H	L	M	H	L	M	H	L	M	H	L	M	H	L	M	H	L	M	H	L	M	H
1367827_at	Ppp2cb	1.1	1.0	1.0	0.9	0.9	1.0	1.1	1.0	1.0	0.9	0.9	1.1	0.9	1.0	1.1	1.0	1.1	1.8	0.9	1.2	2.1	1.0	1.2	2.2
1367831_at	Tp53	1.1	1.2	1.2	0.9	0.8	1.0	1.0	0.9	0.9	0.9	1.0	1.1	1.3	1.0	1.3	1.3	1.3	2.0	1.3	1.0	2.4	0.8	1.2	2.0
1367856_at	G6pdx	0.9	1.2	4.8	1.1	1.6	13	1.3	1.5	2.8	1.0	1.0	1.1	1.4	0.8	1.4	0.5	0.9	1.8	1.1	1.2	3.9	1.0	0.8	5.0
1367890_at	Casp2	1.0	0.8	0.8	1.0	0.8	0.9	0.9	1.1	0.8	0.9	1.0	1.1	1.1	1.0	1.0	1.1	1.2	1.3	0.9	1.0	1.2	1.1	1.1	1.9
1367922_at	Adam17	1.0	1.1	0.9	1.0	1.1	1.5	1.1	1.2	1.8	1.0	1.0	1.1	1.1	0.9	1.0	1.1	1.1	1.0	1.1	0.9	1.1	1.1	1.1	1.7
1368118_at	Bcl10	0.9	0.9	1.0	1.0	0.9	0.8	1.0	0.8	0.9	0.9	1.1	1.1	1.1	0.9	1.0	0.9	0.9	1.6	0.9	1.0	1.6	1.1	1.3	1.8
1368305_at	Casp6	1.1	1.0	1.0	0.7	0.9	0.8	0.8	0.8	0.9	0.9	0.9	1.0	1.3	1.0	1.4	1.0	0.9	1.1	1.0	1.1	1.1	0.9	1.1	1.8
1368544_a_at	Nol3	1.2	1.8	3.1	2.2	3.2	13	1.2	1.0	2.5	2.2	1.5	4.3	1.4	1.4	1.4	1.5	1.0	2.9	1.3	1.5	7.5	0.6	2.5	10
1368856_at	Jak2	1.1	1.1	1.0	1.1	0.9	1.1	1.0	1.1	1.1	1.3	1.2	1.3	1.3	1.0	1.1	1.0	1.1	1.6	1.0	0.8	2.4	0.9	1.1	3.9
1368862_at	Akt1	0.5	0.7	0.9	0.8	1.4	1.6	1.9	3.7	4.5	1.1	1.2	1.4	0.9	0.8	0.9	1.0	0.9	1.3	1.0	1.0	1.6	0.8	1.0	1.4
1368888_a_at	Rtn4	1.1	1.0	1.1	0.9	1.2	1.9	1.1	1.3	1.9	1.1	0.9	1.1	1.3	0.9	1.0	0.9	1.8	2.5	1.3	1.8	2.7	0.8	1.7	4.2
1369104_at	Prkaa1	1.2	1.3	1.8	0.9	1.3	2.6	1.4	1.2	1.3	1.0	0.7	1.0	0.9	1.1	1.3	0.7	0.8	1.6	0.9	1.4	2.1	1.0	1.5	2.0
1369122_at	Bax	1.1	1.1	1.1	0.9	1.1	1.1	1.0	0.9	1.1	1.0	1.0	1.2	1.0	0.9	1.2	1.2	1.4	3.7	0.8	1.1	3.3	0.8	1.6	4.3
1369948_at	Ngfrap1	1.0	1.0	1.0	1.0	1.0	1.0	1.0	0.9	1.3	0.9	1.0	1.4	1.3	1.7	1.7	0.7	1.1	12	1.5	1.7	37	0.9	4.5	63
1369958_at	Rhob	1.0	1.4	2.9	1.2	1.2	3.4	1.2	1.0	2.2	1.1	1.1	2.7	0.9	1.0	1.1	1.0	1.1	2.0	1.2	1.3	3.0	1.0	1.5	3.9
1369995_at	Faf1	0.9	0.9	0.9	1.0	1.0	1.0	1.0	1.1	1.1	1.1	0.9	1.1	1.0	1.0	1.0	1.0	1.0	1.3	0.9	0.9	1.2	1.0	1.0	1.6
1370080_at	Hmox1	0.8	0.9	1.0	1.0	1.0	1.2	1.0	0.8	0.8	1.1	0.8	1.3	1.2	1.0	1.0	1.1	1.1	1.7	1.2	1.4	2.1	0.9	1.1	2.5
1370113_at	Birc3	1.0	1.0	1.1	0.8	1.2	1.1	1.2	0.9	1.2	1.1	1.1	1.2	1.3	0.9	1.2	0.9	0.9	1.1	0.7	0.9	1.4	1.0	1.2	1.9
1370141_at	Mcl1	0.9	1.0	1.0	1.0	1.0	1.1	1.0	0.9	0.9	1.0	1.1	1.3	1.1	1.1	1.2	1.0	1.2	1.5	1.1	1.2	1.4	0.9	1.0	1.6
1370226_at	Cstb	0.9	1.0	1.7	1.0	1.0	3.9	1.2	1.1	1.9	0.8	0.7	0.9	1.2	1.0	1.1	0.9	1.2	1.4	1.0	1.2	2.0	1.0	1.1	2.4
1370243_a_at	Ptma	0.9	0.8	0.9	1.1	1.0	0.9	0.9	0.7	0.8	1.0	1.2	1.2	1.0	0.9	1.0	1.0	1.0	1.3	0.9	1.0	1.5	0.9	1.1	1.7
1370290_at	Tubb5	1.0	1.1	1.2	0.9	1.1	1.4	1.0	1.1	1.1	0.9	0.9	1.0	1.1	1.1	1.1	0.8	0.8	1.3	0.9	0.9	1.8	1.1	1.2	2.6
1370695_s_at	Trib3	0.9	1.1	0.9	1.2	1.5	3.7	1.1	1.3	3.1	1.3	1.5	1.9	1.0	6.5	27	9.8	21	137	1.1	13	77	2.6	8.0	40
1371572_at	App	1.1	0.9	0.9	1.2	1.4	2.5	1.1	1.5	4.2	1.0	1.4	2.9	1.1	1.0	1.4	1.1	1.4	5.0	1.1	1.7	8.0	1.0	2.3	8.9
1373733_at	Bok	0.9	0.9	0.9	0.9	1.0	1.1	1.1	1.2	1.2	0.9	1.0	1.4	1.2	1.0	1.1	1.2	1.0	1.1	1.0	1.0	2.2	1.0	1.1	3.5
1386866_at	Ywhag	1.1	1.0	1.1	1.0	1.0	1.1	1.1	1.0	1.1	1.0	1.0	1.2	1.0	1.0	1.2	1.1	1.2	1.7	1.0	1.1	1.8	1.0	1.2	2.2
1387021_at	Wig1	1.0	1.1	1.1	1.1	1.1	1.7	1.1	1.1	1.6	0.9	0.9	1.2	1.1	1.0	1.1	0.9	1.0	1.5	1.1	1.1	2.3	1.2	1.3	3.4
1387087_at	Cebpb	0.9	1.0	1.0	1.2	1.3	0.7	0.6	0.8	0.7	0.6	0.6	1.7	1.3	1.5	1.3	1.5	1.2	1.6	0.9	1.3	1.6	0.7	1.1	0.8
1387502_at	Stk17b	1.1	1.3	1.4	0.9	1.0	1.9	1.3	1.1	1.1	0.8	1.0	1.1	1.2	1.1	1.2	1.2	1.2	1.6	1.0	1.0	1.5	0.9	1.1	2.0
1387605_at	Casp12	1.0	1.1	1.0	0.9	1.0	1.4	1.1	0.9	1.2	0.9	0.6	1.0	1.3	1.0	1.5	1.2	1.1	1.7	1.8	2.6	5.3	0.4	0.9	1.6
1387818_at	Casp11	2.5	2.3	1.3	1.2	1.0	1.0	0.8	0.9	0.7	1.3	1.7	2.9	1.1	0.9	1.5	1.1	1.2	3.3	1.4	1.7	7.4	0.6	1.6	4.5
1388099_a_at	Tfpt	0.8	0.9	0.9	1.0	1.0	1.0	1.1	0.9	1.0	1.3	1.8	1.6	0.9	0.8	1.1	0.9	0.9	1.4	0.9	1.1	1.9	1.1	1.3	2.6
1388120_at	Pdcd6ip	0.7	2.0	8.0	0.9	3.9	14	2.7	2.9	8.5	1.4	0.6	16	1.0	1.0	1.2	0.9	1.0	1.3	1.0	1.0	1.5	0.9	1.0	1.6
1388674_at	Cdkn1a	1.0	1.1	1.0	0.9	1.0	1.0	0.9	1.0	1.5	1.0	1.3	2.0	1.1	1.0	1.5	0.9	1.5	2.1	1.2	1.8	2.1	0.8	1.9	1.7
1388805_at	Ppp2ca	0.9	0.8	0.9	0.9	1.0	1.1	0.9	0.9	1.1	0.9	1.1	1.1	1.2	1.1	1.5	0.9	1.0	1.7	0.8	1.0	2.7	1.1	1.3	3.6
1388867_at	MGC112830	0.9	1.1	1.2	1.2	1.3	1.7	1.0	1.2	1.6	0.8	0.8	1.0	1.0	1.1	1.1	0.9	1.1	1.3	1.0	1.0	1.2	0.9	1.0	1.7
1389170_at	Casp7	1.0	1.1	1.2	0.9	1.0	0.9	1.0	0.8	1.1	1.3	1.0	1.0	1.0	1.0	1.1	1.0	1.1	1.3	1.0	1.0	1.5	1.1	1.2	1.8
1398948_at	Tax1bp1	0.8	0.8	0.8	1.2	1.0	0.9	1.3	1.0	1.3	1.3	1.8	2.1	1.0	1.1	1.2	1.1	1.2	1.5	1.0	1.1	1.5	1.1	1.1	1.7

The number in each column expresses the ratio to control (N=3).

Fig. 4. Heatmap of individual gene expression change in category of "apoptosis".

of the promising candidates of biomarker genes for oxidative stress-mediated DNA damage, since it was reported to be up-regulated specifically by stress-inducing DNA damage (Corcoran *et al.*, 2005).

It was reported that hepatotoxicity of MP was due to its active metabolite(s) and that oxidative stress was involved (Ratra *et al.*, 1998). However, these authors excluded the involvement of glutathione depletion followed by oxidative stress in the later paper (Ratra *et al.*, 2000). We measured hepatic glutathione contents in rats treated with MP in a separate study (Uehara *et al.*, submitted). Immediately after MP dosing, a transient decrease, not statistically significant, was noted and a rebound-like increase was evident at 24 hr after dosing, which persisted for one week. The increment of glutathione contents disappeared till 2 weeks and it turned to a marked decrease after 4 weeks. These results suggest that MP causes oxidative stress in consuming glutathione while the hepatocytes defend against it by gene expression changes to keep a high glutathione level. Finally, glutathione depletion occurs when the toxicity of MP persists for a long period. We have extracted marker genes for hepatic glutathione depletion using a glutathione depletor, phorone (Kiyosawa *et al.*, 2007). Also in this work, phorone caused a transient decrease of glutathione with a peak at 3 to 6 hr after dosing followed by a rebound-like increase 24 hr after dosing. Taken together, the key of hepatotoxicity of MP is considered to be oxidative damage of DNA followed by changes in MAPK signaling and cell cycle induced by excess production of active metabolites. Sustained oxidative damage of DNA and stimulation of cell proliferation is closely related to hepatocarcinogenesis of MP.

The main purpose of the toxicogenomics approach was to analyze the mechanism of toxicity and predict chronic toxicity from acute data in the preclinical study. In the present study, we simulated the prediction of the toxicity

AFFYMETRIX PROBE ID	SYMBOL	03H			06H			09H			24H			04D			08D			15D			29D		
		L	M	H	L	M	H	L	M	H	L	M	H	L	M	H	L	M	H	L	M	H	L	M	H
1367577_at	Hspb1	1.0	0.9	0.6	1.3	1.4	1.4	0.6	0.8	1.0	1.2	1.3	2.0	1.2	1.5	1.1	1.4	1.3	2.9	0.9	1.3	3.1	0.9	1.6	2.9
1367624_at	Atf4	1.0	1.2	1.8	0.9	1.3	2.2	1.5	1.4	2.2	1.0	0.9	1.3	1.1	1.1	1.3	1.2	1.2	1.6	0.9	1.1	2.0	1.1	1.0	2.0
1367760_at	Map2k1	1.0	1.1	1.1	1.0	1.0	1.1	0.9	0.9	1.0	1.0	1.1	1.2	1.0	1.0	1.3	1.0	1.0	2.0	1.0	1.1	3.1	0.9	1.2	3.7
1367831_at	Tp53	1.0	0.9	0.9	1.0	1.0	1.0	1.0	1.1	1.3	1.1	1.3	1.2	1.3	1.0	1.3	1.3	1.3	2.0	1.3	1.0	2.4	0.8	1.2	2.0
1367890_at	Casp2	1.1	1.1	1.1	0.9	1.1	1.1	1.0	0.9	1.1	1.0	1.0	1.2	1.1	1.0	1.0	1.1	1.2	1.3	0.9	1.0	1.2	1.1	1.1	1.9
1368247_at	Hspa1a / 1b	0.9	1.2	1.4	1.4	1.4	2.6	1.1	1.1	1.5	1.5	1.7	1.8	1.2	1.1	1.8	1.5	1.5	1.4	0.8	1.2	1.2	0.7	0.6	0.4
1368273_at	Mapk6	1.1	1.2	1.2	1.0	1.3	1.8	1.0	1.1	1.4	1.1	1.0	1.0	0.9	0.9	0.9	0.9	0.9	1.1	1.0	0.9	1.1	0.9	1.0	1.0
1368277_at	Ppp3ca	1.1	0.9	1.0	0.9	0.9	1.2	1.2	1.2	1.2	1.1	1.1	1.2	1.0	1.1	1.1	1.0	1.3	1.3	1.1	1.0	1.3	1.2	1.1	1.6
1368305_at	Casp6	0.9	0.9	0.9	0.9	1.0	1.1	1.1	1.2	1.2	0.9	1.0	1.4	1.3	1.0	1.4	1.0	0.9	1.1	1.0	1.1	1.1	0.9	1.1	1.8
1368308_at	Myc	2.0	2.1	3.9	0.7	0.8	3.6	0.7	1.1	1.8	0.8	0.8	1.4	2.0	1.5	1.8	1.5	1.6	2.8	1.9	2.4	5.1	0.9	1.4	3.4
1368862_at	Akt1	1.0	0.8	0.8	1.0	0.8	0.9	0.9	1.1	0.8	0.9	1.0	1.1	0.9	0.8	0.9	1.0	0.9	1.3	1.0	1.0	1.6	0.8	1.0	1.4
1368871_at	Map3k1	1.3	1.0	1.0	0.8	0.7	0.7	0.8	1.2	1.2	0.8	0.7	0.7	0.9	0.9	0.8	0.9	1.0	2.0	1.0	1.2	2.4	1.1	1.0	3.0
1368947_at	Gadd45a	1.3	1.3	5.3	0.6	0.7	2.5	0.8	0.9	1.2	0.8	0.9	1.8	1.1	0.8	1.4	1.1	1.3	3.4	0.6	1.3	3.7	1.5	2.1	7.6
1369590_a_at	Ddit3	1.0	1.3	4.3	1.1	1.1	3.0	1.1	0.9	1.3	1.0	1.1	1.2	0.9	1.0	1.2	0.7	1.0	3.0	0.9	1.2	5.3	1.1	1.3	7.1
1369653_at	Tgfbr2	1.0	1.0	0.9	0.6	0.9	0.7	0.8	1.7	1.5	1.1	1.1	1.0	1.3	1.1	1.4	1.1	1.2	6.5	0.8	2.0	3.2	0.8	1.7	3.2
1369932_a_at	Raf1	1.0	1.1	1.1	1.0	1.2	1.6	1.2	1.2	1.6	0.9	0.9	1.0	1.0	1.1	1.0	0.9	0.9	1.1	1.0	0.9	1.2	0.9	0.9	1.2
1370035_at	Kras2	0.9	0.9	0.8	1.1	1.2	1.5	1.1	1.2	1.5	1.0	0.9	1.1	1.0	1.1	1.0	1.0	1.0	1.3	0.9	1.0	1.2	0.9	1.0	1.3
1370265_at	Arrb2	0.8	0.9	1.2	1.2	1.1	1.1	0.6	1.0	0.8	0.8	0.8	1.2	1.2	1.1	1.1	1.0	1.4	2.4	1.0	0.8	1.6	0.8	1.2	3.2
1370427_at	Pdgfa	0.9	0.8	0.9	1.5	2.4	4.2	1.0	0.9	2.0	0.8	0.7	1.2	1.2	1.1	1.1	2.6	2.5	5.4	0.8	2.0	4.5	0.9	1.0	4.1
1370585_a_at	Prkcb1	0.9	1.0	1.1	1.0	0.9	1.2	1.3	1.0	1.0	0.8	0.9	1.3	1.5	0.9	0.9	0.9	1.0	1.4	1.0	1.0	1.4	1.1	1.2	2.2
1370825_a_at	Cdc42	1.0	0.9	1.0	1.0	1.1	1.0	1.1	1.1	1.1	1.0	1.0	1.1	1.0	1.1	1.1	1.0	1.0	1.3	1.0	1.1	1.5	1.0	1.1	1.5
1370968_at	Nfkb1	1.0	0.9	1.0	1.0	1.0	1.2	1.0	1.0	1.2	1.0	0.8	1.1	1.1	0.9	1.0	1.0	1.0	1.3	1.2	1.1	1.9	1.0	1.2	2.0
1372982_at	Ppp3r1	0.9	1.3	1.3	1.1	1.3	1.5	1.4	1.2	1.2	0.9	1.0	1.2	1.0	1.1	1.0	0.9	0.9	1.5	0.9	0.7	1.1	1.1	1.2	2.2
1375043_at	Fos	0.4	0.3	3.6	0.5	1.0	3.4	2.8	1.7	3.0	0.2	0.2	0.2	0.8	0.8	0.6	1.5	5.5	14	0.5	1.0	6.8	1.8	1.7	15
1376425_at	Tgfb2	1.2	1.1	1.0	1.1	1.4	1.0	1.2	1.0	1.0	1.2	1.3	1.2	1.1	1.0	1.0	1.0	0.9	1.6	1.1	1.1	2.1	1.1	1.3	2.8
1386935_at	Nr4a1	1.1	1.0	1.4	1.1	1.0	1.5	0.7	0.8	0.8	1.1	1.0	1.0	1.2	1.0	1.0	0.9	0.9	1.4	1.0	1.0	1.5	1.1	1.5	2.7
1387377_a_at	Pak1	0.7	0.8	0.9	1.6	1.3	1.5	0.5	0.3	0.6	0.5	0.8	0.9	1.4	0.8	1.2	1.5	0.8	1.4	0.9	2.2	5.1	0.4	0.7	2.8
1387498_a_at	Fgfr1	1.0	0.8	1.0	0.7	0.9	0.7	0.9	1.0	0.9	1.0	1.0	0.9	1.0	1.1	0.9	1.5	1.4	1.9	1.0	1.0	1.3	0.8	1.0	2.3
1387643_at	Fgf21	1.2	2.1	8.8	0.6	1.2	3.6	0.7	1.0	1.6	1.0	1.1	5.1	1.1	1.5	3.9	1.1	5.0	7.5	0.9	4.8	6.4	3.1	3.5	6.6
1387771_a_at	Mapk3	1.2	1.2	1.1	1.1	1.0	0.9	0.9	1.1	0.9	1.1	0.9	1.0	1.2	1.2	1.0	0.9	1.1	1.2	0.9	0.9	1.3	0.9	0.9	2.1
1387806_at	Rap1b	1.0	1.0	1.0	1.0	1.0	1.2	1.0	1.0	1.1	0.9	0.9	1.1	1.1	1.0	1.0	1.0	1.1	1.3	1.0	1.0	1.4	1.0	1.1	1.6
1389170_at	Casp7	1.0	0.9	0.9	0.9	1.0	0.8	0.9	1.0	1.0	1.0	1.0	1.2	1.0	1.0	1.1	1.0	1.1	1.3	1.0	1.0	1.5	1.1	1.2	1.8
1389528_s_at	Jun	1.3	1.3	3.4	0.9	0.6	2.0	0.8	0.8	1.5	0.9	0.5	0.9	1.5	1.5	1.3	1.7	1.4	2.3	0.7	1.4	1.6	1.4	1.4	2.8
1398240_at	Hspa8	0.9	1.3	1.2	1.0	1.1	1.6	1.2	1.2	1.5	1.2	1.2	1.2	1.0	1.0	1.2	1.0	1.1	1.1	0.9	0.9	1.2	0.9	0.9	1.1
1398256_at	Il1b	0.7	0.6	0.6	0.8	0.6	0.8	0.9	0.9	1.1	0.6	0.7	1.1	2.3	0.8	1.5	1.2	1.1	1.5	1.0	1.1	1.8	1.2	1.0	2.1

The number in each column expresses the ratio to control (N=3).

Fig. 5. Heatmap of individual gene expression change in category of "MAPK signaling".

Gene expression in methapyrilene-treated rat liver.

AFFYMETRIX PROBE ID	SYMBOL	03H			06H			09H			24H			04D			08D			15D			29D		
		L	M	H	L	M	H	L	M	H	L	M	H	L	M	H	L	M	H	L	M	H	L	M	H
1367590_at	Ran	1.1	0.9	0.9	1.0	1.1	1.5	1.0	1.1	1.8	1.0	1.3	1.7	0.9	1.0	1.3	1.1	1.2	2.4	1.0	1.2	1.9	1.0	1.4	1.9
1367764_at	Ccng1	0.9	1.0	1.0	1.0	1.2	2.4	1.0	0.9	1.9	1.3	1.3	2.2	0.8	0.9	1.3	1.0	1.1	2.4	1.0	1.0	3.4	1.3	2.2	6.2
1367827_at	Ppp2cb	1.0	1.1	0.9	1.0	1.1	1.5	1.1	1.2	1.8	1.0	1.0	1.1	0.9	1.0	1.1	1.0	1.1	1.8	0.9	1.2	2.1	1.0	1.2	2.2
1367831_at	Tp53	1.0	0.9	0.9	1.0	1.0	1.0	1.0	1.1	1.3	1.1	1.3	1.2	1.3	1.0	1.3	1.3	1.3	2.0	1.3	1.0	2.4	0.8	1.2	2.0
1368076_at	Vhl	1.0	1.1	1.1	1.0	1.0	1.1	1.0	0.9	1.1	1.0	0.9	1.0	1.1	1.0	1.0	1.0	1.1	1.4	1.0	1.0	1.6	1.0	1.0	1.9
1368308_at	Myc	2.0	2.1	3.9	0.7	0.8	3.6	0.7	1.1	1.8	0.8	0.8	1.4	2.0	1.5	1.8	1.5	1.6	2.8	1.9	2.4	5.1	0.9	1.4	3.4
1368947_at	Gadd45a	1.3	1.3	5.3	0.6	0.7	2.5	0.8	0.9	1.2	0.8	0.9	1.5	1.1	0.8	1.4	1.1	1.3	3.4	0.6	1.3	3.7	1.5	2.1	7.6
1369590_a_at	Ddit3	1.0	1.3	4.3	1.1	1.1	3.0	1.1	0.9	1.3	1.0	1.1	1.2	0.9	1.0	1.2	0.7	1.0	3.0	0.9	1.2	5.3	1.1	1.3	7.1
1369932_a_at	Raf1	1.0	1.1	1.1	1.0	1.2	1.5	1.2	1.2	1.6	0.9	0.9	1.0	1.0	1.1	1.0	0.9	0.9	1.1	1.0	0.9	1.2	0.9	0.9	1.2
1369950_at	Cdk4	1.0	1.0	0.9	1.1	1.1	1.1	1.1	1.2	1.3	1.0	1.0	1.2	1.0	1.0	1.1	0.9	1.2	2.0	1.0	1.1	1.9	1.0	1.3	2.2
1369958_at	Rhob	0.9	1.0	1.7	1.0	1.0	3.9	1.2	1.1	1.9	0.8	0.7	0.9	0.9	1.0	1.1	1.0	1.1	2.0	1.2	1.3	3.0	1.0	1.5	3.9
1370035_at	Kras2	0.9	0.9	0.8	1.1	1.2	1.5	1.1	1.2	1.5	1.0	0.9	1.1	1.0	1.1	1.0	1.0	1.0	1.3	0.9	1.0	1.2	0.9	1.0	1.3
1370361_at	Cgref1	1.1	0.6	1.1	0.7	1.0	1.1	0.7	0.9	1.4	0.5	0.6	1.4	1.6	1.9	1.6	1.3	2.0	5.4	0.7	1.2	3.3	1.5	2.3	6.5
1370427_at	Pdgfa	0.9	0.8	0.9	1.5	2.4	4.2	1.0	0.9	2.0	0.8	0.7	1.2	1.2	1.1	1.1	2.6	2.5	5.4	0.8	2.0	4.5	0.9	1.0	4.1
1370504_a_at	Pmp22	1.2	1.5	1.2	0.8	0.9	1.1	0.7	0.7	0.6	0.8	0.8	1.0	1.2	1.4	1.3	1.3	1.6	1.6	1.1	1.3	1.5	1.8	1.4	2.7
1370809_at	Tubg1	1.1	1.0	0.9	1.0	1.0	1.1	1.0	0.9	1.0	1.0	1.0	1.4	1.1	1.2	1.1	1.1	1.0	1.5	0.9	1.2	2.2	1.2	1.5	2.6
1371308_at	Rps4x	1.0	1.0	1.0	0.9	1.0	1.0	1.0	1.0	1.1	1.0	1.1	1.2	1.0	1.0	1.1	1.0	1.1	1.5	1.1	1.3	1.5	1.2	1.3	1.5
1374956_at	Pcm1	1.2	0.9	1.1	0.9	0.9	0.9	1.3	1.1	1.2	1.0	1.1	1.0	1.0	0.9	0.9	1.2	1.2	1.4	1.0	0.9	1.3	1.1	0.9	1.6
1375630_at	RGD:1303103	1.0	0.8	1.0	1.0	1.1	1.3	1.1	1.0	1.4	1.0	1.1	1.3	0.9	1.0	1.0	1.2	1.2	1.6	1.1	1.2	1.9	1.0	1.2	1.8
1376425_at	Tgfb2	1.2	1.1	1.0	1.1	1.4	1.0	1.2	1.0	1.0	1.2	1.3	1.2	1.1	1.0	1.0	1.0	0.9	1.6	1.1	1.1	2.1	1.1	1.3	2.8
1379375_at	Pdgfa	1.1	1.1	1.1	1.0	1.2	2.0	0.9	0.9	1.6	0.7	0.8	1.1	1.2	1.1	1.3	0.8	1.0	1.9	0.9	0.9	2.1	1.1	1.3	3.0
1386866_at	Ywhag	1.1	1.0	1.1	0.9	1.2	1.5	1.1	1.3	1.9	1.1	0.9	1.1	1.0	1.0	1.2	1.1	1.2	1.7	1.0	1.1	1.8	1.0	1.2	2.2
1387391_at	Cdkn1a	0.9	1.1	0.9	1.1	1.5	3.9	0.6	0.7	2.8	1.2	2.2	2.9	1.2	1.1	1.4	1.9	2.5	5.9	1.1	2.1	3.1	0.9	2.8	2.5
1387616_at	Pdgfc	1.0	1.0	0.9	1.0	0.9	1.2	1.1	1.0	0.8	1.0	0.9	0.8	1.2	0.8	1.1	1.3	1.3	1.6	0.9	0.9	1.2	0.8	0.9	2.2
1387644_at	Btc	1.0	1.1	1.0	1.1	0.9	0.9	1.0	0.9	0.7	0.9	1.1	1.1	1.3	1.0	1.4	1.3	0.8	1.0	0.9	1.0	1.6	1.0	0.8	1.9
1387788_at	Junb	1.2	1.0	1.6	1.1	0.7	1.3	0.7	0.9	1.5	1.6	1.4	1.4	1.4	0.9	1.4	1.1	1.0	1.3	1.0	1.1	2.1	1.1	1.0	4.0
1388154_at	E2f5	1.0	1.0	1.1	1.0	1.4	1.7	1.0	1.1	1.7	1.2	1.1	1.2	1.0	1.0	1.1	1.1	1.1	1.4	1.0	1.0	1.5	0.9	1.1	1.7
1388805_at	Ppp2ca	1.1	1.0	1.0	1.1	1.0	1.4	1.1	1.0	1.4	0.9	1.0	1.5	1.2	1.1	1.5	0.9	1.0	1.7	0.8	1.0	2.7	1.1	1.3	3.6
1388867_at	MGC112830	1.0	1.1	1.2	0.9	1.1	1.4	1.0	1.1	1.1	0.9	0.9	1.0	1.0	1.1	1.1	0.9	1.1	1.3	1.0	1.0	1.2	0.9	1.0	1.7
1389101_at	Ccnc	0.7	0.7	0.5	0.9	1.1	1.2	1.2	1.0	0.8	1.2	1.1	1.4	1.2	1.1	1.1	1.1	1.3	2.0	1.3	1.6	2.5	1.5	1.6	2.5
1389528_s_at	Jun	1.3	1.3	3.4	0.9	0.6	2.0	0.8	0.8	1.5	0.9	0.5	0.9	1.5	1.5	1.3	1.7	1.4	2.3	0.7	1.4	1.6	1.4	1.4	2.8
1398240_at	Hspa8	0.9	1.3	1.2	1.0	1.1	1.6	1.2	1.2	1.5	1.2	1.2	1.2	1.0	1.0	1.2	1.0	1.1	1.1	0.9	0.9	1.2	0.9	0.9	1.1
1398256_at	Il1b	0.7	0.6	0.6	0.8	0.6	0.8	0.9	0.9	1.1	0.6	0.7	1.1	2.3	0.8	1.5	1.2	1.1	1.5	1.0	1.1	1.8	1.2	1.0	2.1

The number in each column expresses the ratio to control (N=3).

Fig. 6. Heatmap of individual gene expression change in category of "regulation of cell cycle".

of MP by focusing on the toxicological pathway drawn from transcriptome analysis. Genes up-regulated from the early stage described above would be promising candidates of biomarkers for hepatotoxicity. However, the present analysis focused on one chemical, MP. It is necessary to analyze other chemicals causing glutathione depletion/oxidative stress and nongenotoxic hepatocarcinogenesis, such as thioacetamide, coumarin and ethionine, in order to establish a useful and precise prediction system based on the toxicogenomics approach.

The greatest advantage of toxicogenomics in toxicology is that various toxicity mechanisms can be elucidated at once compared with the conventional strategy where many experiments are performed one by one. This strategy is so powerful that comprehensive seizure of what happens for the mechanism in the target organ is possible. Toxicogenomics enables one to supply supporting data for any conventional toxicological changes and suggests the appropriate toxicological mechanism behind them.

ACKNOWLEDGMENT

This work was supported in part by a grant from the Ministry of Health, Labour and Welfare (H14-Toxico-001).

REFERENCES

Althaus, F.R., Lawrence, S.D., Sattler, G.L. and Pitot, H.C. (1982): DNA damage induced by the antihistaminic drug methapyrilene hydrochloride. Mutat. Res., **103**, 213-218.

Chu, T.M., Deng, S., Wolfinger, R., Paules, R.S. and Hamadeh, H.K. (2004): Cross-site comparison of gene expression data reveals high similarity. Environ. Health Perspect., **112**, 449-455.

Corcoran, C.A., Luo, X., He, Q., Jiang, C., Huang, Y. and Sheikh, M.S. (2005): Genotoxic and endoplasmic reticulum stresses differentially regulate TRB3 expression. Cancer Biol. Ther., **4**, 1063-1067.

Fischer, G., Altmannsberger, M., Schauer, A. and Katz, N. (1983): Early stages of chemically induced liver carcinogenesis by oral administration of the antihistaminic methapyrilene hydrochloride. J. Cancer Res. Clin. Oncol., **106**, 53-57.

Hamadeh, H. K., Knight, B.L., Haugen, A.C., Sieber, S., Amin, R.P.,

Bushel, P.R., Stoll, R., Blanchard, K., Jayadev, S., Tennant, R.W., Cunningham, M.L., Afshari, C.A. and Paules, R.S. (2002): Methapyrilene toxicity: Anchorage of pathologic observations to gene expression alterations. Toxicol. Pathol., **30**, 470-482.

Kiyosawa, N., Shiwaku, K., Hirode, M., Omura, K., Uehara, T., Shimizu, T., Mizukawa, Y., Miyagishima, T., Ono, A., Nagao, T. and Urushidani, T. (2006): Utilization of a one-dimensional score for surveying the chemical-induced changes in expression levels of multiple biomarker gene sets using a large-scale toxicogenomics database. J. Toxicol. Sci., **31**, 433-448.

Kiyosawa, N., Uehara, T., Gao, W., Omura, K., Hirode, M., Shimizu, T., Mizukawa, Y., Ono, A., Miyagishima, T., Nagao, T. and Urushidani, T. (2007): Identification of glutathione depletion-responsive genes using phorone-treated rat liver. J.Toxicol. Sci., **32**, 469-486.

Lijinsky, W., Reuber, M.D. and Blackwell, B.N. (1980): Liver tumors induced in rats by oral administration of the antihistaminic methapyrilene hydrochloride. Science, **209**, 817-819.

Mirsalis, J.C. (1987): Genotoxicity, toxicity, and carcinogenicity of the antihistamine methapyrilene. Mutat. Res., **185**, 309-317.

NTP Hepatotoxicity Studies of the Liver Carcinogen Methapyrilene Hydrochloride (CAS No. 135-23-9) Administered in Feed to Male F344/N Rats. Toxic Rep Ser. 46:1-C7, 2000.

Ratra, G.S., Morgan, W.A., Mullervy, J., Powell, C.J. and Wright, M.C. (1998): Methapyrilene hepatotoxicity is associated with oxidative stress, mitochondrial disfunction and is prevented by the Ca^{2+} channel blocker verapamil. Toxicology, **130**, 79-93.

Ratra, G.S., Powell, C.J., Park, B.K., Maggs, J.L. and Cottrell, S. (2000): Methapyrilene hepatotoxicity is associated with increased hepatic glutathione, the formation of glucuronide conjugates, and enterohepatic recirculation. Chem. Biol. Interact., **129**, 279-295.

Snedecor, G.W. and Cochran, W.G. (1989): Statistical Methods, 8th ed., Iowa State University Press.

Steinmetz, K.L., Tyson, C.K, Meierhenry, E.F., Spalding, J.W, and Mirsalis, J.C. (1988): Examination of genotoxicity, toxicity and morphologic alterations in hepatocytes following *in vivo* or *in vitro* exposure to methapyrilene. Carcinogenesis, **9**, 959-963.

Turner, N.T., Woolley, J.L. Jr., Hozier, J.C., Sawyer, J.R. and Clive, D. (1987): Methapyrilene is a genotoxic carcinogen: Studies on methapyrilene and pyrilamine in the L5178Y/TK +/– mouse lymphoma assay. Mutat. Res., **189**, 285-297.

Urushidani, T. and Nagao, T. (2005): Toxicogenomics: The Japanese initiative. In Handbook of Toxicogenomics - Strategies and Applications. (Borlak, J., ed.), pp. 623-631. Wiley-VCH.

Waring, J.F., Ulrich, R.G., Flint, N., Morfitt, D., Kalkuhl, A., Staedtler, F., Lawton, M., Beekman, J.M. and Suter, L. (2004): Interlaboratory evaluation of rat hepatic gene expression changes induced by methapyrilene. Environ. Health Perspect., **112**, 439-448.

Human & Experimental Toxicology (2008) 27: 23–35
www.het.sagepub.com

Species-specific differences in coumarin-induced hepatotoxicity as an example toxicogenomics-based approach to assessing risk of toxicity to humans

T Uehara[1], N Kiyosawa[1], T Shimizu[1], K Omura[1], M Hirode[1], T Imazawa[1], Y Mizukawa[2], A Ono[1], T Miyagishima[1], T Nagao[3] and T Urushidani[1,2]

[1]Toxicogenomics Project, National Institute of Biomedical Innovation, Ibaraki, Osaka, Japan; [2]Department of Pathophysiology, Faculty of Pharmaceutical Sciences, Doshisha Women's College of Liberal Arts, Kyotanabe, Kyoto, Japan; and [3]National Institute of Health Sciences, Setagaya-ku, Tokyo, Japan

One expected result from toxicogenomics technology is to overcome the barrier because of species-specific differences in prediction of clinical toxicity using animals. The present study serves as a model case to test if the well-known species-specific difference in the toxicity of coumarin could be elucidated using comprehensive gene expression data from rat in-vivo, rat in-vitro, and human in-vitro systems. Coumarin 150 mg/kg produced obvious pathological changes in the liver of rats after repeated administration for 7 days or more. Moreover, 24 h after a single dose, we observed minor and transient morphological changes, suggesting that some early events leading to hepatic injury occur soon after coumarin is administered to rats. Comprehensive gene expression changes were analyzed using an Affymetrix GeneChip® approach, and differentially expressed probe sets were statistically extracted. The changes in expression of the selected probe sets were further examined in primary cultured rat hepatocytes exposed to coumarin, and differentially expressed probe sets common to the in-vivo and in-vitro datasets were selected for further study. These contained many genes related to glutathione metabolism and the oxidative stress response. To incorporate human data, human hepatocyte cultured cells were exposed to coumarin and changes in expression of the bridging gene set were examined. In total, we identified 14 up-regulated and 11 down-regulated probe sets representing rat–human bridging genes. The overall responsiveness of these genes to coumarin was much higher in rats than humans, consistent with the reported species difference in coumarin toxicity. Next, we examined changes in expression of the rat–human bridging genes in cultured rat and human hepatocytes treated with another hepatotoxicant, diclofenac sodium, for which hepatotoxicity does not differ between the species. Both rat and human hepatocytes responded to the marker genes to the same extent when the same concentrations of diclofenac sodium were exposed. We conclude that toxicogenomics-based approaches show promise for overcoming species-specific differences that create a bottleneck in analysis of the toxicity of potential therapeutic treatments.

Key words: coumarin; hepatocyte; hepatotoxicity; human; liver; rat; toxicogenomics

Introduction

The Toxicogenomics Project (TGP) is a 5-year collaborative project of the National Institute of Health Sciences, the National Institute of Biomedical Innovation, and 15 pharmaceutical companies in Japan that began in 2002.[1] The aim was to construct a large-scale toxicology database of transcriptomes useful to predict the toxicity of new chemical entities in early stages of drug development. About 150 chemicals, primarily medicinal compounds, were selected and gene expression in the rat liver (also kidney in some cases) or rat and human hepatocytes was comprehensively analyzed by using the Affymetrix GeneChip®.[2] In 2007, the project was completed and the whole system, consisting of a database, an analysis system, and a prediction system, was completed and named TG-GATEs (for Genomics Assisted Toxicity Evaluation System developed by Toxicogenomics Project in Japan).

Correspondence to: Tetsuro Urushidani, Department of Pathophysiology, Faculty of Pharmaceutical Sciences, Doshisha Women's College of Liberal Arts, Kodo, Kyotanabe, Kyoto 610-0395, Japan. Email: turushid@dwc.doshisha.ac.jp

10.1177/0960327107087910

The main purpose of creating the system was to facilitate analysis of the mechanisms of toxicity and prediction of chronic toxicity from acute data in preclinical studies, and the consensus response to the project is that toxicogenomics-based technologies provide a useful tool. However, the final goal of a preclinical study should be prediction of clinical toxicity based on animal data. Toward this end, overcoming species-specific differences has proved to be the most difficult problem. We expect that elucidation of mechanisms of toxicity using toxicogenomics-based tools should lead to an improved ability to use animal data to make reasonable predictions of toxicity in humans.[3] However, there have been few reports of species-specific differences in the toxicological response at the level of changes in gene expression.[4]

We obtained gene expression data from rat primary hepatocytes as well as human frozen hepatocytes (in addition to rat in-vivo liver) to build an informational bridge between the two species. In the present study, we analyzed the effects of coumarin, a representative hepatotoxicant with a known species-specific difference in toxicity, as a model case for determining if species-specific differences in hepatotoxicity can be accurately predicted using a toxicogenomics-based approach.

Materials and methods

Chemicals

Coumarin and diclofenac sodium (DFNa) were obtained from Tokyo Chemical Industry (Tokyo, Japan).

Animal Treatment

All experimental protocols using animals were reviewed and approved by the Ethics Review Committee for Animal Experimentation of the National Institute of Health Sciences. The experimental protocols using human hepatocytes were reviewed and approved by both the Ethics Review Committees for Experimentation on Human Subjects of the National Institute of Health Sciences and of the National Institute of Biomedical Innovation.

Five-week-old male Sprague-Dawley rats were obtained from Charles River Japan Inc. (Kanagawa, Japan). After a 7-day quarantine and acclimatization period, 6-week-old animals were assigned to dosage groups (five rats per group) using a computerized stratified random grouping method based on individual body weight. The animals were individually housed in stainless-steel cages in an animal room that was lighted for 12 h (7:00–19:00) daily, ventilated with an air-exchange rate of 15 times per hour and maintained at 21–25 °C with a relative humidity of 40–70%. Each animal was allowed free access to water and pellet diet (CRF-1, sterilized by radiation; Oriental Yeast Co., Ltd., Tokyo, Japan).

Either vehicle (corn oil), or 15, 50, or 150-mg/kg coumarin was administered orally to rats once daily on day 1, 3, 7, 14, and 28, and the animals were euthanized 24 h after the last dosing by exsanguination from the abdominal aorta under ether anesthesia. Liver samples were obtained from the left lateral lobe of the liver of each animal immediately after sacrifice. For light microscopy, liver samples were fixed in 10% neutral-buffered formalin, dehydrated in alcohol, and embedded in paraffin. Paraffin sections were prepared and stained using standard methods for hematoxylin and eosin staining. Histopathological findings were graded into four categories: very slight, slight, moderate, and severe. For electron microscopy, a piece of tissue from the liver was fixed in 2.5% glutaraldehyde solution. Ultra-thin sections, stained with Mayer's hematoxylin and lead citrate after standard tissue processing, were observed under a Hitachi electron microscope (H-7650; Hitachi High-Technologies Corporation Tokyo, Japan).

Hepatocyte treatment

Hepatocytes were isolated from 6-week-old male Sprague-Dawley rats under sodium pentobarbital (120 mg/kg, i.p.) and anesthetized using a modified two-step collagenase perfusion method. The liver was perfused via the portal vein for 10 min with divalent, cation-free, EGTA (ethylene glycol-bis[β-aminoethyl ether]-N,N,N',N'-tetraacetic acid) (0.5 mM)-supplemented HEPES (4-(2-hydroxyethyl)-1-piperazineethanesulfonic acid)-buffered Hank's balanced salt solution followed by a 10-min perfusion with HEPES (10 mM)-buffered normal Hank's balanced salt solution containing soybean trypsin inhibitor (0.05 g/L, T-2011; Sigma Aldrich, St Louis, Missouri, USA) and collagenase (0.5 g/L, 034-10533; Wako Pure Chemical Industries, Osaka, Japan) at a flow rate of 10–30 mL/min. The isolated cells were washed three times and centrifugated at $50 \times g$ for 1 min to obtain a parenchymal cell-enriched pellet. Hepatocytes were not used when their viability was <70% (as assessed by trypan blue exclusion). Cell samples that passed the threshold for viability were seeded into collagen-coated six-well plates (BD BioCoat™ Collagen I Cellware; BD Bioscience, Bedford, Massachusetts, USA) at a density of 1×10^6 cells/well in 2 mL HMC Bulletkit medium (Cambrex,

Walkersville, Maryland, USA) supplemented with 10% fetal bovine serum.

For human hepatocytes (Tissue Transformation Technologies Inc., presently BD Biosciences, San Jose, California, USA), the frozen cells were thawed, washed twice with medium (L15 medium supplemented with penicillin, streptomycin, and 10% fetal bovine serum), and then seeded as described for rat hepatocytes except that the cell density was 1.2×10^6 cells/well.

Following an attachment period of 3 h, the medium was replaced and kept overnight before exposure to the drug at 37 °C in an atmosphere of 5% CO_2. The test compounds were added to the medium directly or as a 1000× stock solution in dimethylsulfoxide (DMSO). After 2, 8, or 24-h exposure, cells were dissolved with RLT buffer (Qiagen, Valencia, California, USA) and collected for expression profiling. GeneChip analysis was performed in duplicate for each concentration.

Cell viability was assessed by monitoring leakage of lactate dehydrogenase (LDH). To do this, both the culture medium and the cell lysate (lysis with 0.1% Triton X-100) were analyzed using an automatic biochemical analyzer (TBA-200FR; Toshiba, Tokyo, Japan) and the rate of survival relative to a control was calculated as follows: $LDH_{cell}/(LDH_{cell} + LDH_{medium})$.

The appropriate concentrations of test drugs were determined in a preliminary experiment. For our general protocol, the highest concentration was set to 10–20% of the lethal concentration as estimated by LDH leakage over 24 h. When the cells could tolerate as much as 10 mM or the level equal to the solubility limit of the compound in DMSO (allowed to add up to 0.1% in the final concentration), the highest concentration was set to either value. Exposures were performed at two different concentrations, 1/5 and 1/25 of the highest concentration. In case of coumarin, no LDH leakage was observed for either rat or human hepatocytes after treatment with concentrations of up to 300 μM, which was the solubility limit. Thus, concentrations of 12, 60, and 300 μM coumarin were used in subsequent assays. For DFNa, 400 μM was set as the maximum both in rats and humans. Thus, concentrations of 16, 80, and 400 μM DFNa were used in subsequent assays.

GeneChip analysis

For analysis of rat livers, microarray analysis was conducted on three of five samples from each single dose group (24-h post-dose) using GeneChip® RAE 230A probe arrays (Affymetrix, Santa Clara, California, USA). Liver samples were homogenized with buffer RLT supplied with the RNeasy Mini Kit (Qiagen) and total RNA was isolated according to the manufacturer's instructions.

For hepatocytes, GeneChip analysis was performed in duplicate for each concentration using RAE230 2.0 probe arrays for rat hepatocytes and U133 Plus 2.0 arrays for human hepatocytes (Affymetrix). Cells were dissolved with RLT buffer and collected for expression profiling. Different versions were used for the in-vitro versus the in-vivo study because RAE230 2.0 was released after the in-vivo experiments were completed. The procedure was conducted basically as described in the manufacturer's instructions using Superscript Choice System (Invitrogen, Carlsbad, California, USA) and T7-(dT)24-oligonucleotide primer (Affymetrix) for cDNA synthesis, cDNA Cleanup Module (Affymetrix) for purification, and BioArray High yield RNA Transcript Labeling Kit (Enzo Diagnostics, Farmingdale, New York, USA) for synthesis of biotin-labeled cRNA. Ten micrograms of fragmented cRNA was hybridized to a RAE230A probe array for 18 h at 45 °C at 60 rpm, after which the array was washed and stained with streptavidin–phycoerythrin using Fluidics Station 400 (Affymetrix) and scanned with a Gene Array Scanner (Affymetrix). The digital image files were processed using Affymetrix Microarray Suite version 5.0. Microarray image data were analyzed with GeneChip Operating Software (Affymetrix). All microarray data were scaled by global normalization with the mean signal intensity of all data adjusted to 500.

Gene expression data analysis

To identify genes that are differentially expressed after in-vivo coumarin treatment, the Student's *t*-test was applied with a P value cut-off of 0.05 in combination with fold changes of 2.0 or greater and 0.5 or less using Spotfire® DecisionSite for Functional Genomics (Spotfire, Göteborg, Sweden). Probe sets designated as absent by an Affymetrix detection call in any of six samples (three each for control and treated) were excluded from further analysis.

To extract genes that changed in response to coumarin in both the in-vivo and in-vitro sample groups, the changes in expression of the above-mentioned probe sets were examined in rat hepatocytes treated with the high dose (300 μM) of coumarin. Probe sets showing 1.5-fold or greater (up-regulated) and 0.6-fold or less (down-regulated) were selected.

In the next step, the genes in common to the in-vivo and in-vitro rat assays were compared in rat versus human hepatocytes. To do this, we first examined public data on human orthologs of the

rat genes (NetAffx[5]). Upon assignment of orthologs, rat probes sets without human ortholog information were excluded. Because for the redundant probe sets for human samples, a single probe set was selected based on the reliability and dose-dependency of the expression profile. Finally, the probe sets, which were designated as absent by Affymetrix detection, call in seven or more out of eight samples (two each for control and high dose treated in rat and human) were excluded from further analysis.

To facilitate analysis in the large-scale microarray database, we developed two types of one-dimensional score, TGP1 and TGP2, which express the trends in changes in expression of biomarker genes as a whole. The former is based on the signal log ratio[6] and is convenient for comparing the responsiveness of several drugs to a marker gene list. The disadvantages of this scoring system are that it overestimates responsiveness when the list contains a gene for which induction is extreme (such as CYP1A1) and it underestimates responsiveness when genes in the list are mobilized in either direction. To overcome these disadvantages, we used another score, TGP2, which is based on the size of the effects $g = l\mu_2 - \mu_1 l/\sigma_{\text{pooled}}$, where

$$\sigma_{pooled} = \sqrt{\frac{(N_1-1)\sigma_1 + (N_2-1)\sigma_2^2}{(N_1+N_2-2)}}$$

To obtain an unbiased estimate of the effect size $d = c \times d$, where c is bias correction[7]

$$c = 1 - \frac{3}{4(N_1+N_2-2)-1}$$

The corrected effect size was calculated for each probe set in the marker gene list, summed, and divided by the number of probe sets in the list, and finally multiplied by 100 to obtain the TGP2 score used in the present study.

Results

Changes in rat livers in response to treatment with coumarin

We noted several pathological changes in rat livers after administration of coumarin (Table 1). Twenty-four hour after a single dose of coumarin, no abnormal morphological changes were observed by light microcopy (Figure 1a,b). However, histopathological changes became apparent with repeated administration of coumarin for 1 week or later in the highest dose group, and degenerative lesions, such as vacuolar degeneration and intracytoplasmic inclusion bodies, were evident at day 29 post-initiation of treatment (Figure 1c,d). From day 4 to day 29, single cell necrosis of hepatocytes was occasionally observed.

We next used electron microscopy to look for subtle changes that may be apparent 24 h after a single dose of coumarin. The analysis showed dilation of the rough endoplasmic reticulum of hepatocytes in

Table 1 Histopathological findings in rat livers treated with coumarin

Histopathological findings	*Time Point (days)*	*2*			*4*			*8*			*15*			*29*		
	Dose (mg/kg)	*15*	*50*	*150*	*15*	*50*	*150*	*15*	*50*	*150*	*15*	*50*	*150*	*15*	*50*	*150*
	Number of animals examined	*5*	*5*	*5*	*5*	*5*	*5*	*5*	*5*	*5*	*5*	*5*	*5*	*5*	*5*	*5*
Hepatocyte / Single cell necrosis		0	0	0	0	0	1	0	0	1	0	0	1	0	0	2
very slight							1			1			1			2
Hepatocyte / Inclusion body, intracytoplasmic		0	0	0	0	0	0	0	0	5	0	0	5	0	0	5
very slight										5			2			
slight													3			2
moderate																3
Hepatocyte, centrilobular / Hypertrophy		0	0	0	0	0	0	0	0	3	0	0	5	0	0	5
very slight										3			2			1
slight													3			4
Hepatocyte, centrilobular / Degeneration, vacuolar		0	0	0	0	0	0	0	0	0	0	0	3	0	0	5
very slight													2			
slight													1			5

Vehicle alone or coumarin 15, 50, or 150 mg/kg was administered orally to rats once daily for 1, 3, 7, 14, and 28 days, and the animals were euthanized 24 h after the last dosing, namely, on 2, 4, 8, 15, and 29 days ($n = 5$). The pathological change in the liver was graded into four categories: very slight, slight, moderate, and severe. The number of animals having the morphology at each grade is shown.

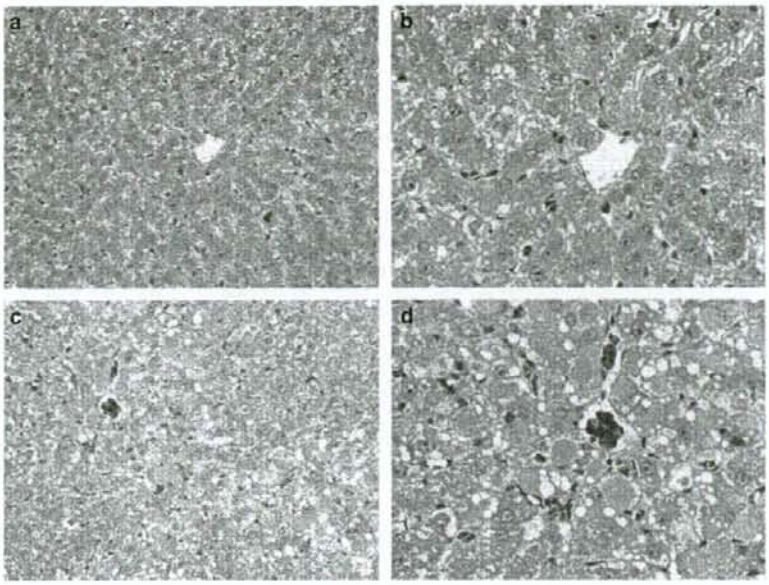

Figure 1 Histopathological changes in the rat liver treated with 150 mg/kg coumarin. (a) Low (×100) and (b) high (×200) magnification micrographs of a liver treated once with 150 mg/kg coumarin (24 h after a single dose). No abnormal morphological changes were detected in the control liver. (c) Low (×100) and (d) high (×200) magnification images of a liver treated with 150 mg/kg coumarin once a day for 28 days. Degenerative changes, such as vacuolation of hepatocytes, are evident after repeated administration of coumarin.

the centrilobular region of the liver in the highest dose group (Figure 2). This early slight ultrastructural change was considered to be consistent with hepatic injury we observed after repeated exposure to the drug. Thus, the 24-h post-treatment time point seemed appropriate for microarray analysis, as at the cellular level, coumarin had already begun exerting an effect at 24-h post-single treatment.

As described in the Methods section, statistically significant up- (136 probe sets) and down-regulated genes (79 probe sets) were extracted and these are listed in Tables 2 and 3. In livers treated with coumarin, the following genes were remarkably mobilized, that is, genes involved in glutathione metabolism and oxidative stress: "glutathione reductase", "glutathione-S-transferase, pi 1/2", "glutathione S-transferase Yc2 subunit", "microsomal glutathione S-transferase 2", "glutamate-cysteine ligase, catalytic subunit", "glutamate-cysteine ligase, modifier subunit", "aldo-keto reductase family 7, member A3

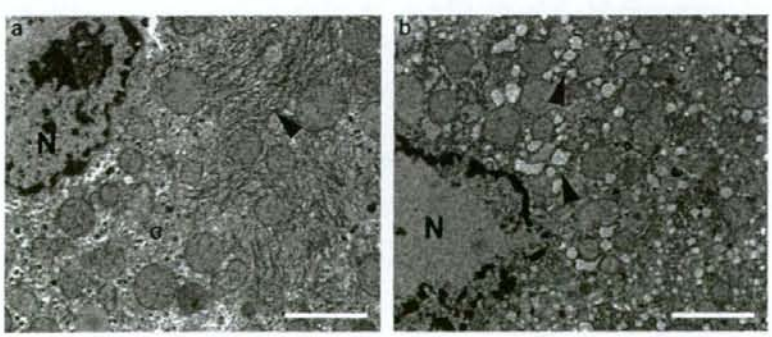

Figure 2 Early detection of coumarin-induced changes by electron microscopy. (a) Control hepatocyte, (b) coumarin-treated hepatocyte (150 mg/kg; 24 h after a single dose). Expansion of the rough endoplasmic reticulum (rER) in the coumarin-treated hepatocyte as compared with a control is evident. N, nucleus; Arrowhead, rER; Bar = 2 μm.

Table 2 Genes up-regulated in the rat liver 24 h after administration of coumarin

Affymetrix probe set ID	*Gene symbol*	*Gene description*	*Fold change*		
			Dose (mg/kg)		
			15	*50*	*150*
1371817_at	LOC290651	Similar to myo-inositol 1-phosphate synthase A1	9.52		26.50
1388122_at	Gstp1/Gstp2	Glutathione-S-transferase, pi 1/pi 2	2.84	1.57	13.00
1369698_at	Abcc3	ATP-binding cassette, sub-family C (CFTR/MRP), member 3	4.41	2.59	11.58
1370342_at	Kcnk2	Potassium channel, subfamily K, member 2	2.45	3.22	10.87
1368013_at	Ddit4l	DNA-damage-inducible transcript 4-like	1.71	1.41	9.07
1388271_at	LOC682651/LOC689415	Similar to Metallothionein-2 (MT-2) (Metallothionein-II) (MT-II)	1.39	1.40	8.81
1375213_at	Pck2_predicted	Phosphoenolpyruvate carboxykinase 2 (mitochondrial) (predicted)	3.07	1.97	6.09
1371237_a_at	Mt1a	Metallothionein 1a	1.52	1.70	5.92
1368121_at	Akr7a3	Aldo-keto reductase family 7, member A3 (aflatoxin aldehyde reductase)	3.43	2.00	5.78
1387599_a_at	Nqo1	NAD(P)H dehydrogenase, quinone 1	2.68	2.33	5.77
1371970_at	RGD1560913_predicted	Similar to expressed sequence AW413625 (predicted)	2.92	1.19	5.67
1371089_at	—	Transcribed locus	2.25	1.38	5.29
1379740_at	LOC361346	Similar to chromosome 18 open reading frame 54	2.29	2.32	4.96
1387693_a_at	Slc6a9	Solute carrier family 6 (neurotransmitter transporter, glycine), member 9	1.66	0.97	4.94
1372510_at	Srxn1	Sulfiredoxin 1 homolog	1.19	0.95	4.91
1370902_at	Akr1b8	Aldo-keto reductase family 1, member B8	2.20	1.96	4.69
1369772_at	Slc6a9	Solute carrier family 6 (neurotransmitter transporter, glycine), member 9	1.45	0.92	4.42
1368247_at	Hspa1a /Hspa1b	Heat shock 70kD protein 1A/1B (mapped)	2.18	1.94	4.22
1387925_at	Asns	Asparagine synthetase	1.40	1.35	4.06
1376051_at	Cryl1	Crystallin, lamda 1	1.25	1.24	3.94
1367847_at	Nupr1	Nuclear protein 1	1.24	1.46	3.86
1368143_at	Anxa7	Annexin A7	1.68	1.38	3.77
1377016_at	Creld2	Cysteine-rich with EGF-like domains 2	0.88	0.94	3.75
1373043_at	LOC680945/LOC683036	Similar to stromal cell–derived factor 2-like 1	1.86	1.99	3.71
1388102_at	Ltb4dh	Leukotriene B4 12-hydroxydehydrogenase	1.44	1.05	3.59
1372653_at	Fkbp11	FK506 binding protein 11	1.64	1.42	3.54
1373810_at	Pla2g12a_predicted	Phospholipase A2, group XIIA (predicted)	1.42	1.96	3.53
1376247_at	—	Transcribed locus	1.97	1.39	3.52
1371442_at	Hyou1	Hypoxia up-regulated 1	1.26	0.88	3.50
1372985_at	Zfp444_predicted	Zinc finger protein 444 (predicted)	2.10	1.28	3.47
1373787_at	Slc6a9	Solute carrier family 6 (neurotransmitter transporter, glycine), member 9	1.35	1.02	3.30
1394080_at	—	Transcribed locus	2.66	2.54	3.17
1373850_at	Smpdl3b	Sphingomyelin phosphodiesterase, acid-like 3B	1.46	1.23	3.07
1370073_at	Dnajc3	Protein kinase inhibitor p58	1.53	1.31	3.06
1374036_at	Mcm2_predicted	Minichromosome maintenance deficient 2 mitotin (predicted)	1.55	0.85	3.06
1370912_at	Hspa1b	Heat shock 70kD protein 1B (mapped)	1.64	1.46	3.01
1377145_at	LOC362068	Similar to monogenic, audiogenic seizure susceptibility 1	1.56	1.63	2.99
1392920_at	Ell3	Elongation factor RNA polymerase II-like 3	1.62	1.41	2.96
1376668_at	RGD1311126_predicted	Similar to RIKEN cDNA 4922503N01 (predicted)	0.92	0.79	2.94
1389308_at	Dnajb11	DnaJ (Hsp40) homolog, subfamily B, member 11	1.42	1.14	2.91
1376055_at	Mcm5_predicted	Minichromosome maintenance deficient 5, cell division cycle 46 (predicted)	1.81	1.07	2.90
1375852_at	Hmgcr	3-hydroxy-3-methylglutaryl-Coenzyme A reductase	1.28	0.91	2.90
1386958_at	Txnrd1	Thioredoxin reductase 1	1.07	0.81	2.89
1371210_s_at	RT1-Aw2	RT1 class Ib, locus Aw2	1.50	1.72	2.88
1372390_at	—	Transcribed locus	1.25	0.81	2.86
1374359_at	Ccne2_predicted	Cyclin E2 (predicted)	1.24	0.91	2.85
1370665_at	Hyou1	Hypoxia up-regulated 1	1.03	0.87	2.84
1387212_at	Bhlhb8	Basic helix-loop-helix domain containing, class B, 8	1.51	2.29	2.81
1374805_at	RGD1561749_predicted	Similar to hypothetical protein MGC5528 (predicted)	2.25	1.13	2.81
1389578_at	Isrip	Ischemia/reperfusion inducible protein	1.23	1.25	2.73
1370429_at	RT1-Aw2	RT1 class Ib, locus Aw2	1.89	1.29	2.70
1370803_at	Zwint	ZW10 interactor	1.58	1.23	2.68
1370688_at	Gclc	Glutamate-cysteine ligase, catalytic subunit	1.06	0.64	2.67
1377037_at	LOC679253/LOC681337	Similar to Acyl-coA thioesterase 4	1.32	0.96	2.65
1375428_at	Creg_predicted	Cellular repressor of E1A-stimulated genes (predicted)	1.24	1.17	2.65
1374048_at	Nrtn	Neurturin	1.61	1.63	2.64
1377334_at	RT1-Ba	RT1 class II, locus Ba	1.86	1.85	2.63

(continued)

Table 2 *(continued)*

Affymetrix probe set ID	*Gene symbol*	*Gene description*	*Fold change*		
			Dose (mg/kg)		
			15	*50*	*150*
1388628_at	Tmed3	Transmembrane emp24 domain containing 3	1.40	1.17	2.59
1367733_at	Ca2	Carbonic anhydrase 2	1.11	0.86	2.59
1373557_at	Mcm4	Minichromosome maintenance deficient 4 homolog	1.51	0.90	2.57
1368544_a_at	Nol3	Nucleolar protein 3	1.30	1.67	2.57
1372954_at	—	Sprague-Dawley UV73 mRNA, partial sequence	1.37	1.80	2.54
1369061_at	Gsr	Glutathione reductase	1.27	1.09	2.53
1370007_at	Pdia4	Protein disulfide isomerase associated 4	1.10	0.98	2.53
1389391_at	RGD1564876_predicted	Similar to solute carrier family 35, member E3 (predicted)	1.26	0.98	2.50
1372523_at	Gclc	Glutamate-cysteine ligase, catalytic subunit	1.17	0.79	2.50
1390591_at	Slc17a3	Na/Pi cotransporter 4	1.67	1.07	2.49
1368376_at	Nr0b2	Nuclear receptor subfamily 0, group B, member 2	1.74	1.69	2.49
1398791_at	Txnrd1	Thioredoxin reductase 1	1.10	0.89	2.48
1367938_at	Ugdh	UDP-glucose dehydrogenase	1.28	0.96	2.46
1387022_at	Aldh1a1	Aldehyde dehydrogenase family 1, member A1	2.15	1.21	2.44
1373613_at	LOC300191	Similar to RIKEN cDNA 4930570C03	1.09	0.96	2.44
1372406_at	Mcm3_predicted	Minichromosome maintenance deficient 3 (predicted)	1.65	0.81	2.43
1374121_at	—	Transcribed locus	2.32	1.82	2.41
1372261_at	—	Transcribed locus	1.23	1.13	2.41
1384130_at	RGD1560171_predicted	Similar to PRO0149 protein (predicted)	1.63	2.13	2.39
1380030_at	Znf593_predicted	Zinc finger protein 593 (predicted)	1.09	0.88	2.38
1389671_at	Trpc2	Transient receptor potential cation channel, subfamily C, member 2	1.21	1.29	2.36
1373445_at	Nol8_predicted	Nucleolar protein 8 (predicted)	1.24	0.85	2.36
1387083_at	Ctf1	Cardiotrophin 1	1.18	0.96	2.35
1377135_at	Alox5	Arachidonate 5-lipoxygenase	1.00	1.25	2.34
1375088_at	—	Transcribed locus	0.98	1.14	2.31
1369588_a_at	Atpif1	ATPase inhibitory factor 1	1.27	1.13	2.30
1398341_at	RGD1559720_predicted	RGD1559720 (predicted)	1.03	1.09	2.29
1389767_at	RGD1304924_predicted	Similar to hypothetical protein FLJ31364 (predicted)	1.13	1.18	2.29
1374249_at	RGD1304580	Similar to Hypothetical protein MGC38513	0.93	1.10	2.28
1373530_at	Ccne1	cyclin E	1.06	0.52	2.28
1371113_a_at	Tfrc	Transferrin receptor	1.28	0.76	2.28
1370127_at	Pold1	Polymerase (DNA directed), delta 1, catalytic subunit	1.42	1.37	2.28
1376073_at	Sel1h	Sel1 (suppressor of lin-12) 1 homolog	1.40	1.06	2.26
1392841_at	—	Transcribed locus	1.39	2.02	2.23
1398879_at	Tmem66	Transmembrane protein 66	1.25	1.07	2.22
1388622_at	Nol5a	Nucleolar protein 5A	1.46	1.19	2.22
1371583_at	Rbm3	RNA binding motif protein 3	1.19	1.16	2.21
1387188_at	Slc17a1	Solute carrier family 17, member 1	1.37	1.33	2.20
1368037_at	Cbr1	Carbonyl reductase 1	0.96	1.01	2.20
1390430_at	Nr1d2	Nuclear receptor subfamily 1, group D, member 2	0.97	1.05	2.19
1398788_at	Pdia3	Protein disulfide isomerase associated 3	1.43	1.24	2.19
1386922_at	Ca2	Carbonic anhydrase 2	1.07	0.83	2.19
1367983_at	Fen1	Flap structure–specific endonuclease 1	1.59	1.12	2.16
1373999_at	—	Transcribed locus	1.27	0.83	2.16
1376781_at	Glb1_mapped	Galactosidase, beta 1 (mapped)	1.20	1.03	2.14
1381968_at	Sema6d_predicted	Sema domain, transmembrane domain (TM), and cytoplasmic domain, (semaphorin) 6D (predicted)	1.18	1.20	2.13
1372774_at	Coq6	Coenzyme Q6 homolog	1.30	0.90	2.13
1376098_a_at	Lad1_predicted	Ladinin (predicted)	1.02	1.03	2.12
1370904_at	Hla-dma	Major histocompatibility complex, class II, DM alpha	1.32	1.11	2.12
1389805_at	—	—	1.27	1.29	2.11
1388331_at	Tra1_predicted	Tumor rejection antigen gp96 (predicted)	1.08	0.93	2.11
1386466_at	—	Transcribed locus	1.08	1.24	2.11
1372599_at	Mgst2_predicted	Microsomal glutathione S-transferase 2 (predicted)	1.34	1.34	2.11
1372471_at	—	Transcribed locus	1.66	1.03	2.10
1372247_at	Ddost_predicted	Dolichyl-di-phosphooligosaccharide-protein glycotransferase (predicted)	1.26	1.15	2.10
1370055_at	Rab3d	RAB3D, member RAS oncogene family	0.72	0.77	2.10
1398596_at	—	Transcribed locus	2.07	1.65	2.09
1387783_a_at	Acaa1	Acetyl-coenzyme A acyltransferase 1	1.49	1.20	2.09
1373908_at	—	—	1.71	1.40	2.09
1398383_at	Cyb561_predicted	Cytochrome b-561 (predicted)	1.40	1.15	2.07
1377350_at	—	Transcribed locus	1.74	1.26	2.07
1370428_x_at	RT1-Aw2	RT1 class Ib, locus Aw2	1.66	1.50	2.07

(continued)

Table 2 *(continued)*

Affymetrix probe set ID	*Gene symbol*	*Gene description*	*Fold change*		
			Dose (mg/kg)		
			15	*50*	*150*
1369693_a_at	Slc1a2	Solute carrier family 1, member 2	1.81	1.96	2.07
1370541_at	Nr1d2	Nuclear receptor subfamily 1, group D, member 2	0.91	1.01	2.06
1389004_at	Josd2_predicted	Josephin domain containing 2 (predicted)	1.12	0.95	2.06
1370030_at	Gclm	Glutamate cysteine ligase, modifier subunit	1.06	0.81	2.06
1370000_at	Thra	Thyroid hormone receptor alpha	1.79	1.66	2.06
1370663_at	Wee1	Wee 1 homolog	1.92	1.00	2.05
1390321_at	RGD1304693_predicted	Similar to CG14803-PA (predicted)	1.68	1.15	2.03
1389209_at	RGD1306274	Similar to hypothetical protein BC002942	1.82	1.17	2.03
1388750_at	Tfrc	Transferrin receptor	1.32	0.87	2.03
1373935_at	Pold2	Polymerase (DNA directed), delta 2, regulatory subunit	1.35	1.18	2.03
1390579_at	RGD1305222_predicted	Similar to RIKEN cDNA 1810029B16 (predicted)	0.84	0.70	2.02
1389889_at	RGD1306404_predicted	Similar to mKIAA1402 protein (predicted)	1.21	1.03	2.02
1373499_at	Gas5	Growth arrest specific 5	1.15	1.03	2.02
1373386_at	Gjb2	Gap junction membrane channel protein beta 2	0.81	1.08	2.02
1376001_at	Praf1_predicted	Polymerase (RNA) I associated factor 1 (predicted)	1.17	0.98	2.01
1373200_at	Eef1e1_predicted	Eukaryotic translation elongation factor 1 epsilon 1 (predicted)	1.19	1.25	2.01
1380854_at	R3hdm1	R3H domain containing 1	1.20	1.28	2.00

Probe sets are sorted by fold change. Shaded probe sets, those selected as in-vivo–in-vitro bridging probes (see Figure 3).

(aflatoxin aldehyde reductase)", "NAD(P)H dehydrogenase, quinone 1", "thioredoxin reductase 1", and "metallothionein"; genes related to the heat shock response: "crystallin, lamda 1", "DnaJ (Hsp40) homolog, subfamily B, member 11", "heat shock 70kD protein 1A/1B", and "protein kinase inhibitor p58"; genes responsive to hypoxia: "hypoxia up-regulated 1" and "ischemia/reperfusion inducible protein"; and genes related to DNA repair and the cell cycle: "DNA-damage-inducible transcript 4-like", "cyclin E", "growth arrest specific 5", and "wee 1 homolog". Changes in expression of these genes in hepatocytes can be interpreted as a reflection of the adaptive response to oxidative stress and cellular damage. Among the extracted genes, the following genes appeared to be the most sensitive to coumarin, "aldo-keto reductase family 7, member A3", "NAD(P)H dehydrogenase, quinone 1", "glutathione reductase", "glutathione-S-transferase, pi 1/2", and "glutathione S-transferase Yc2 subunit", as they were remarkably mobilized at the lowest dose of coumarin-treatment (15 mg/kg).

Comparison between in-vivo and in-vitro rat hepatocyte responses

Primary cultured rat hepatocytes were exposed to 12, 60, and 300 μM coumarin for 24 h. No obvious cytotoxicity was detected by LDH release (100.5, 97.7, and 95.1% of control, respectively). In case of the in-vitro system, statistical filtering was not appropriate because the data were the duplicate measurements from a single rat. We then extracted the significant genes according to the gene list obtained from in-vivo study, that is, the genes showing significant up- (136 probe sets) or down-regulation (79 probe sets) in livers treated with 150 mg/kg coumarin. As shown in Figure 3a, a similar trend was observed between in-vivo and in-vitro cell responses, although the extent of the response (i.e., fold change) was generally smaller, and fewer genes showed a measurable change in the in-vitro cell assay. Probe sets showing changes of 1.5-fold or more and 0.6-fold or less than that of control at the highest concentration (300 μM) in rat hepatocytes were selected as those reflecting the toxicological mechanism of coumarin *in vivo*, namely, "in-vivo–in-vitro bridging probes". For the selected genes (37 up-regulated and 29 down-regulated; see shading in Tables 2 and 3), clear dose-dependent changes in expression were observed (Figure 3b), and the observation enabled us to assess hepatotoxicity of coumarin using the in-vitro data.

Comparison between rat and human hepatocytes

Cultured human hepatocytes were also exposed to 12, 60, and 300 μM coumarin for 24 h. No obvious cytotoxicity was detected by LDH release (100.6, 100.9, and 102.0% of control, respectively). The in-vivo–in-vitro bridging probes were assigned to their human ortholog genes to form a set of "rat–human bridging probes" and changes in their expression were compared in rat versus human hepatocytes. In total, 14 up-regulated and 11 down-regulated probe sets were identified and their relative expression levels are shown as a heatmap in Figure 4. It appears that the pattern of changes in gene expres-

Table 3 Genes down-regulated in the rat liver 24 h after administration of coumarin

Affymetrix probe set ID	*Gene symbol*	*Gene description*	*Fold change*		
			Dose (mg/kg)		
			15	*50*	*150*
1386977_at	Ca3	Carbonic anhydrase 3	0.64	1.01	0.13
1370778_at	LOC259245	Alpha-2u globulin	0.87	0.84	0.16
1386474_at	—	Transcribed locus	1.53	0.59	0.19
1393902_at	Akr1c6	Aldo-keto reductase family 1, member C6	0.42	0.53	0.20
1375900_at	LOC500590	Similar to T-cell antigen 4-1BB precursor – mouse	0.56	0.52	0.21
1371412_a_at	Nrep	Neuronal regeneration related protein	0.86	0.88	0.25
1387491_at	Gyk	Glycerol kinase	0.76	0.72	0.28
1376637_at	—	Transcribed locus	0.62	1.03	0.29
1373722_at	Kif20a_predicted	Kinesin family member 20A (predicted)	1.12	0.91	0.29
1367896_at	Ca3	Carbonic anhydrase 3	0.80	0.98	0.29
1385247_at	Ugt2b	UDP glycosyltransferase 2 family, polypeptide B	0.68	0.04	0.31
1387852_at	Thrsp	Thyroid hormone–responsive protein	1.06	0.87	0.32
1393221_at	RGD1564865_predicted	Similar to 20-alpha-hydroxysteroid dehydrogenase (predicted)	0.67	0.97	0.32
1387665_at	Bhmt	Betaine-homocysteine methyltransferase	0.81	1.18	0.33
1387185_at	Apbb3	Amyloid beta (A4) precursor protein-binding, family B, member 3	0.84	0.84	0.33
1387053_at	Fmo1	Flavin containing monooxygenase 1	0.62	0.79	0.34
1398286_at	Csad	Cysteine sulfinic acid decarboxylase	1.07	0.92	0.34
1387655_at	Cxcl12	Chemokine (C-X-C motif) ligand 12	0.67	0.45	0.34
1368458_at	Cyp7a1	Cytochrome P450, family 7, subfamily a, polypeptide 1	0.78	0.69	0.36
1388583_at	Cxcl12	Chemokine (C-X-C motif) ligand 12	0.77	0.67	0.37
1387243_at	Cyp1a2	Cytochrome P450, family 1, subfamily a, polypeptide 2	0.78	0.90	0.37
1387139_at	Hao2	Hydroxyacid oxidase 2 (long chain)	0.79	1.15	0.37
1373006_at	Prp2	Proline-rich protein PRP2	0.70	0.79	0.37
1370026_at	Cryab	Crystallin, alpha B	1.01	0.71	0.37
1390443_at	—	Transcribed locus	0.88	0.75	0.38
1375144_at	—	Transcribed locus	1.02	0.52	0.39
1369044_a_at	Pde4b	Phosphodiesterase 4B	0.59	0.64	0.39
1370057_at	Csrp1	Cysteine and glycine-rich protein 1	0.93	0.90	0.39
1369450_at	Ust5r	Integral membrane transport protein UST5r	0.74	0.94	0.39
1367729_at	Oat	Ornithine aminotransferase	0.63	1.00	0.39
1374677_at	LOC684425	Similar to adenylosuccinate synthetase isozyme 1	0.80	1.00	0.40
1388038_at	Atrn	Attractin	0.88	0.88	0.40
1388031_x_at	LOC259245/Mup5	Alpha-2u globulin	0.70	0.95	0.40
1370150_a_at	Thrsp	Thyroid hormone–responsive protein	1.03	0.97	0.41
1390450_a_at	Ogn_predicted	Osteoglycin (predicted)	0.63	0.53	0.41
1369664_at	Avpr1a	Arginine vasopressin receptor 1A	0.88	0.87	0.41
1388433_at	Krt1-19	Keratin complex 1, acidic, gene 19	1.09	0.71	0.42
1371400_at	Thrsp	Thyroid hormone–responsive protein	1.04	0.98	0.42
1369296_at	Sult1c1	Sulfotransferase family, cytosolic, 1C, member 1	0.86	1.13	0.42
1389728_at	—	—	0.77	0.56	0.42
1389188_at	Gpr108	G protein-coupled receptor 108	0.69	0.53	0.42
1380546_at	LOC298250	Similar to hypothetical protein FLJ10986	0.87	0.89	0.42
1376427_a_at	Gldc_predicted	Glycine decarboxylase (predicted)	0.85	0.88	0.42
1372685_at	Cdkn3_predicted	Cyclin-dependent kinase inhibitor 3 (predicted)	1.03	1.14	0.42
1369546_at	Bbox1	Butyrobetaine (gamma), 2-oxoglutarate dioxygenase 1	0.90	0.82	0.42
1389566_at	Ccnb2	Cyclin B2	1.13	1.11	0.43
1374157_at	Rgs8	Regulator of G-protein signaling 8	0.76	0.61	0.43
1398282_at	Kynu	Kynureninase (L-kynurenine hydrolase)	0.73	0.96	0.44
1387816_at	Igfals	Insulin-like growth factor binding protein, acid labile subunit	1.09	0.77	0.45
1387528_at	Mbl2	Mannose binding lectin 2, protein C	0.77	0.86	0.45
1387372_at	Slc6a13	Solute carrier family 6, member 13	0.89	0.75	0.45
1376311_at	RGD1563465_predicted	Similar to netrin G1 (predicted)	0.79	0.29	0.45
1374072_at	LOC689898	Hypothetical protein LOC689898	0.97	0.62	0.45
1370355_at	Scd1	Stearoyl-coenzyme A desaturase 1	1.56	1.13	0.45
1368627_at	Rgn	Regucalcin	0.85	0.91	0.45
1387203_at	Gckr	Glucokinase regulatory protein	0.79	1.01	0.46
1388425_at	RGD1305890	Similar to RIKEN cDNA D130038B21	0.83	0.78	0.46
1377412_at	—	Transcribed locus	0.91	0.67	0.46
1377375_at	Aass_predicted	Aminoadipate-semialdehyde synthase (predicted)	0.98	0.80	0.46
1374760_at	—	Transcribed locus	0.76	1.07	0.46
1373967_at	—	Transcribed locus	0.87	0.77	0.46
1367979_s_at	Cyp51	Cytochrome P450, subfamily 51	0.92	0.77	0.46
1367939_at	Rbp1	Retinol binding protein 1, cellular	0.62	0.90	0.46

(continued)